Enriched finite elements and local rescaling for vibrations of axially inhomogeneous Timoshenko beams

Rémi Cornaggia, Eric Darrigrand, Loïc Le Marrec, Fabrice Mahé

Enriched finite elements and local rescaling for vibrations of axially inhomogeneous Timoshenko beams

R. Cornaggia[a,*], E. Darrigrand[b], L. Le Marrec[b], F. Mahé[b]

[a] *Laboratoire de mécanique et d'acoustique, UMR 7031 CNRS-AMU-École Centrale, Marseille, France*
[b] *Université de Rennes, CNRS, IRMAR - UMR 6625, F-35000 Rennes, France*

Abstract

This work presents a new enriched finite element method dedicated to the vibrations of axially inhomogeneous Timoshenko beams. This method relies on the "half-hat" partition of unity and on an enrichment by solutions of the Timoshenko system corresponding to simple beams with a homogeneous or an exponentially-varying geometry. Moreover, the efficiency of the enrichment is considerably increased by introducing a new formulation based on a local rescaling of the Timoshenko problem. Validations using analytical solutions and comparisons with the classical high-order polynomial FEM, conduced for several inhomogeneous beams, show the efficiency of this approach in the time-harmonic domain. In particular low error levels are obtained over large ranges of frequencies using fixed coarse meshes. Possible extensions to the research of natural frequencies of beams and to simulations of transient wave propagation are highlighted.

Keywords: Vibrations; Inhomogeneous Timoshenko beams; Enriched finite elements

1. Introduction

The Timoshenko model is widely used to describe the bending of beams, especially for vibration or wave propagation problems, as it approaches the dispersion relations of realistic 3D beams much more accurately than the simpler Rayleigh or Euler-Bernoulli models for medium and high frequencies [12, 11]. Numerous analytical and numerical methods based on this model have therefore been designed to address these problems, see *e.g.* the review by Hajianmaleki and Qatu [14].

Many of these works focus on homogeneous beams, but attention has also been dedicated to various geometrically or materially heterogeneous beams. Beams whose cross-section varies along the axial direction were studied from the 90' [6, 34, 38], and this direction of research has been recently revived by the interest on periodically varying structures and the dynamic features (dispersion, band-gaps ...) they induce [21, 37]. Moreover, the interest in composite materials, exhibiting continuously varying effective material parameters at the macroscopic level, lead to numerous studies of the so-called *functionally graded beams* (FGBs). These works propose several ways to take into account a material heterogeneity in the transverse direction [1], in the axial direction [25], or in both directions [35]. Ultimately, beams that are both geometrically and materially heterogeneous are also considered [26, 15, 5].

In this work, we focus on geometrically heterogeneous beams submitted to time-harmonic loads. Indeed, results in the time-harmonic regime provide a basis for eigenfrequency search, time-domain simulations or modal analysis of beams [22], and a method dedicated to geometrical heterogeneities in the axial direction can easily be extended to axially functionally graded beams. Moreover, closed-form time-harmonic solutions of the Timoshenko system are only available for simple exponential or polynomial variations of the cross-section area and quadratic momentum [8, 25, 33, 36]. More complex heterogeneities thus require suitable numerical methods.

*Corresponding author.
Email addresses: cornaggia@lma.cnrs-mrs.fr (R. Cornaggia), eric.darrigrand-lacarrieu@univ-rennes1.fr (E. Darrigrand), loic.lemarrec@univ-rennes1.fr (L. Le Marrec), fabrice.mahe@univ-rennes1.fr (F. Mahé)

Among many available methods [14], the traditional finite element method (FEM) [9, 16] featuring low-order polynomial shape functions is a reliable choice for static or low-frequency problems and slowly varying heterogeneities. To tackle higher frequencies and sharper inhomogeneities, two improvements are often considered: (i) using higher-order polynomial shape functions [32], the resulting method being sometimes called the *hp*-FEM or *spectral* FEM [18, 30], or (ii) *enriching* the finite element basis with problem-related functions chosen to approximate the exact solution better than polynomials. This second approach is adopted in this paper.

More specifically, we base our work on the partition of unity method (PUM) by Melenk and Babuška [20] and its descendant the generalized FEM [31] (see also the historical introduction provided by Babuška and Banerjee [3]). The PUM and related methods have already been applied to Timoshenko beams, *e.g.* to get rid of the "locking effect" that occur for very thin beams when using traditional FEM, for static loadings [19, 4, 23] or vibrations [27]. In these studies, the enrichment functions are often chosen either as particular solutions of the static Timoshenko system for homogeneous beams, even when the focus is on the vibrations of heterogeneous beams as in [38, 26], or as oscillating functions whose design relies on numerical considerations rather than physical ones [27].

Based on these works, to increase the efficiency of PUM-base enrichment methods, we develop an approach that lies on two main components: use of new enrichment functions and new formulation of the Timoshenko problem.

On the one hand, we consider new families of enrichment functions that tackle both the heterogeneity of the beam and the time-harmonic nature of the motion, developing a procedure introduced in our preliminary work [7] that addresses the scalar Webster's equation. This procedure features (i) a flexible "half-hat" partition of unity, and (ii) enrichment functions chosen as the solutions of the time-harmonic Timoshenko system for homogeneous or exponentially varying beams. Moreover, its implementation is identical to the one of the classical ninth-order polynomial FEM and therefore it can be incorporated in existing codes with reasonable implementation effort, and the static condensation procedure [16, 7] can be applied.

On the other hand, an original local rescaling (*i.e.* a position-dependent change of unknowns) is introduced to obtain a new formulation of the Timoshenko problem, which can also be discretized using the same enriched FEM. This formulation partially accounts for the heterogeneity effects, thus the new unknowns are less affected by the heterogeneity, and therefore are much better approximated by the chosen enrichment functions.

The resulting method is first validated using the analytical solutions available for homogeneous and exponentially varying beams, and for boundary and distributed loadings. To show the efficiency of our method to handle the inhomogeneity of the beam, several numerical experiments and comparisons with the reference ninth-order polynomial FEM are then conduced on four beams with increasing complexity of inhomogeneity. We display the results obtained with the following four configurations: (i) standard ninth-order polynomial FEM (ii) enriched FEM, (iii) local rescaling and polynomial FEM and (iv) local rescaling and enriched FEM. They assert the efficiency of combining the two proposed ingredients (configuration (iv)), especially for medium and high frequencies for which low error levels can still be obtained with very coarse meshes.

The paper is organized as follows. Section 2 presents the problems we consider, and gathers notations and existing results used throughout the paper. Section 3 briefly recalls the features of the FEM for Timoshenko beams and describes our enrichment procedure. We introduce the change of unknowns and the associated problem formulation in Section 4. The numerical validations and examples are then presented in Section 5. Finally, we conclude and highlight the perspectives of this work in Section 6.

2. Notations and available exact solutions to the Timoshenko system

Throughout the paper, we consider a beam of length $\bar{L}$, submitted to in-plane time-harmonic loading at circular frequency $\bar{\omega}$, *i.e.* forces and momentums whose time dependency, omitted hereafter, is $e^{-\mathrm{i}\bar{\omega}\bar{t}}$. Following the Timoshenko theory [12], the resulting in-plane motion is described by the time-harmonic transverse displacement of the mean axis (taken here as the $\bar{x}$-axis) and the rotation of the cross-section (Figure 1), whose amplitudes $\bar{u}$ and θ are solutions of the system:

$$\begin{cases} \dfrac{d}{d\bar{x}}\left(\kappa GA\left(\dfrac{d\bar{u}}{d\bar{x}}-\theta\right)\right)+\rho A\bar{\omega}^2\bar{u}+\bar{q}=0 \\ \dfrac{d}{d\bar{x}}\left(EI\dfrac{d\theta}{d\bar{x}}\right)+\kappa GA\left(\dfrac{d\bar{u}}{d\bar{x}}-\theta\right)+\rho I\bar{\omega}^2\theta+\bar{m}=0, \end{cases} \tag{1}$$

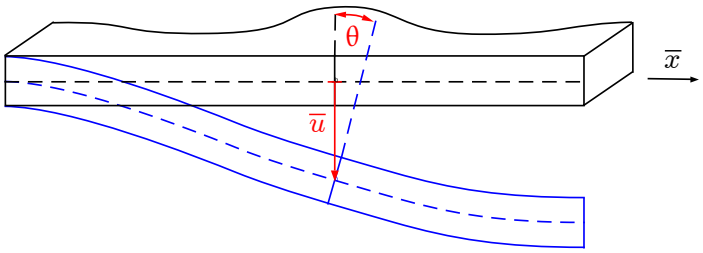

Figure 1: Bending of a geometrically heterogeneous beam: notation.

where ρ, G and E are respectively the density, the shear modulus and Young's modulus of the constitutive material of the beam; A and I are the area and quadratic momentum of the cross-section; κ is the shear correction factor, which depends on the shape of the cross-section [13, 32]; and $\bar{q}$ and $\bar{m}$ are the spatial amplitudes of time-harmonic linear densities of forces and moments, respectively. In these equations, the shear force $\bar{N}$ and the bending moment $\bar{M}$ have been expressed in terms of the kinematic variables $(\bar{u}, \theta)$ thanks to the classical linear elastic constitutive relations $\bar{N} = \kappa GA(d\bar{u}/d\bar{x} - \theta)$ and $\bar{M} = EI(d\theta/d\bar{x})$.

Since we consider geometrically heterogeneous beams made of a homogeneous constitutive material, the geometrical parameters A and I depend on $\bar{x}$, while the material parameters ρ, G and E are uniform. To simplify ensuing computations, we additionally assume that the shape of the cross-section varies sufficiently slowly so that the correction factor κ can also be considered uniform.

To complete the system (1), two boundary conditions (BCs) must be imposed at each extremity of the beam, each pair of conditions corresponding to a kind of support. Classical examples of these supports include the glued extremity ($\bar{u} = 0$ and $\theta = 0$); the simply supported extremity ($\bar{u} = 0$ and $\bar{M} = 0$); the vertical roller connection ($\bar{N} = 0$ and $\theta = 0$); and the free extremity ($\bar{N} = 0$ and $\bar{M} = 0$).

2.1. Dimensionless Timoshenko system

For further convenience, the system (1) is now reformulated into a dimensionless form, similarly to *e.g.* [10, 29]. To this end, constant characteristic amplitudes A_c and I_c are introduced. These will be chosen as $A_c = A(0)$ and $I_c = I(0)$ thereafter, but other choices are possible, *e.g.* A_c and I_c may be the mean values of A and I along the beam. Then, the relevant scales of the problem are the gyration radius r_c, Timoshenko's cut-off frequency ω_c, and the shear-compression ratio g defined by:

$$r_c = \sqrt{\frac{I_c}{A_c}}, \qquad \omega_c = \frac{1}{r_c}\sqrt{\frac{G}{\rho}}, \qquad g = \frac{E}{\kappa G}. \tag{2}$$

In particular, for most materials, one has $2 \lesssim g \lesssim 3$. Dimensionless counterparts of the coordinate, parameters, fields and unknowns that appear in the system (1) are defined thanks to these scales as:

$$x = \frac{\bar{x}}{r_c}, \quad L = \frac{\bar{L}}{r_c}, \quad u = \frac{\bar{u}}{r_c}, \quad \omega = \frac{\bar{\omega}}{\omega_c}, \quad q = \frac{\bar{q} r_c}{\kappa G A_c} \quad \text{and} \quad m = \frac{\bar{m} r_c^2}{\kappa G I_c}. \tag{3}$$

We similarly define the dimensionless and strictly positive functions $\mathcal{A}$ and $\mathcal{I}$, that we call *profiles* of the area and quadratic momentum, as:

$$\mathcal{A}(x) = \frac{A(\bar{x})}{A_c} \qquad \text{and} \qquad \mathcal{I}(x) = \frac{I(\bar{x})}{I_c}. \tag{4}$$

Combining the definitions (3) and (4) with the original system (1), one founds that the couple of dimensionless unknowns (u, θ) satisfies:

$$\begin{cases} \big(\mathcal{A}(u' - \theta)\big)' + \omega^2 \mathcal{A} u + q = 0 \\ g\,(\mathcal{I}\theta')' + \mathcal{A}(u' - \theta) + \omega^2 \mathcal{I}\theta + m = 0 \end{cases} \tag{5}$$

where $'$ stands for differentiation with respect to the dimensionless coordinate x. By analogy with the system (1), we also define the dimensionless shear force N and bending moment M as:

$$N = \mathcal{A}(u' - \theta) \quad \text{and} \quad M = g\mathcal{I}\theta', \tag{6}$$

so that $N(x) = \bar{N}(\bar{x})/\kappa G A_c$ and $M(x) = r_c \bar{M}(\bar{x})/\kappa G I_c$. Boundary conditions must finally be applied on the couples (u, θ), (u, M), (N, θ) or (N, M) at both extremities, $x = 0$ and $x = L$, to complete the problem.

Remark 1. *The Timoshenko system can often be reduced to only one fourth-order equation. For geometrically heterogeneous beams and when no linear density of forces is applied ($q = 0$), it was pointed out by Huang et al. [15] that the displacement u and rotation θ may be both written in terms of a new unknown function f as:*

$$u = \frac{f'}{\mathcal{A}}, \qquad \theta = \left(\frac{f'}{\mathcal{A}}\right)' + \omega^2 \frac{f}{\mathcal{A}}. \tag{7}$$

Then the shear force is $N = \mathcal{A}(u' - \theta) = -\omega^2 f$ and the transverse equilibrium equation $N' + \omega^2 \mathcal{A} u = 0$ is automatically verified. The rotation equilibrium equation becomes a fourth-order equation in f:

$$\left(\mathcal{I}\left[\left(\frac{f'}{\mathcal{A}}\right)' + \omega^2 \frac{f}{\mathcal{A}}\right]'\right)' + \omega^2 \left(\mathcal{I}\left[\left(\frac{f'}{\mathcal{A}}\right)' + \omega^2 \frac{f}{\mathcal{A}}\right] - f\right) + m = 0. \tag{8}$$

However, we prefer to work with the classical system (5)*, as (i) it enables to consider nonzero density of forces q (ii) the boundary conditions involving θ or M are more easily expressed and (iii) the corresponding weak formulation of the problem (see Section 3.1) is posed in the usual functional space $H^1(0, L)$ whereas a weak formulation obtained from the fourth-order equation* (8) *would be posed in $H^2(0, L)$ and the choice of a finite element basis would therefore be more constrained.*

2.2. Available exact solutions for free vibrations

We end this section by providing some exact solutions available in the literature for the free vibrations of Timoshenko beams, *i.e.* solutions of the system (5) with $q = 0$ and $m = 0$. These solutions will be used to build enriched finite element spaces in the next section, and to validate the whole method in Section 5.

Homogeneous beams. For a homogeneous beam, $\mathcal{A}$ and $\mathcal{I}$ are uniform and the only remaining geometrical parameter of the problem is the constant $\alpha := \mathcal{A}/\mathcal{I}$. The system (5) becomes:

$$\begin{cases} (u' - \theta)' + \omega^2 u = 0 \\ g\theta'' + \alpha(u' - \theta) + \omega^2 \theta = 0 \end{cases} \tag{9}$$

Then, looking for oscillating solutions as classically done [12], with the same wavenumber k for u and θ, *i.e.* $u(x) = u_0 e^{\mathrm{i}kx}$ and $\theta(x) = \theta_0 e^{\mathrm{i}kx}$, one obtains the dispersion relation:

$$gK^2 - \omega^2(g + 1)K + \omega^2(\omega^2 - \alpha) = 0, \quad \text{with} \quad K := k^2, \tag{10}$$

which admits two real solutions:

$$K_\pm = \frac{\omega^2(g + 1) \pm \omega\sqrt{4g\alpha + \omega^2(g - 1)^2}}{2g}. \tag{11}$$

The four values that can be taken by the wavenumber k are therefore:

$$k_1 = \sqrt{K_+}, \quad k_2 = -\sqrt{K_+}, \quad k_3 = \sqrt{K_-}, \quad k_4 = -\sqrt{K_-}, \tag{12}$$

These wavenumbers are represented in Figure 2 as ω increases. Note in particular that $K_+ > 0$, so that k_1 and k_2 are real, whereas K_- has the same sign as $\omega - \sqrt{\alpha}$, so that k_3 and k_4 are imaginary at low frequencies [11]. For high frequencies, one has $K_+ \sim \omega^2$ and $K_- \sim \omega^2/g$ as $\omega \to \infty$, regardless of the value of α.

Finally, the basis of solutions for the Timoshenko system (9), parametrized by α, is:

$$\Psi^{\omega,\alpha} = \left\{x \mapsto e^{\mathrm{i}k_m x}\right\}_{m=1..4}. \tag{13}$$

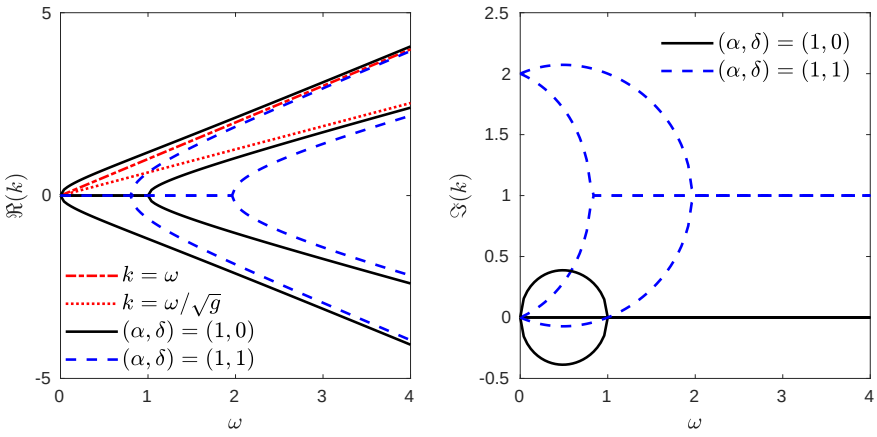

Figure 2: Dispersion relations for homogeneous and exponentially varying beams: real (left) and imaginary (right) parts of the wavenumbers $k_m(\omega)$ (solid) and $\widehat{k}_m(\omega)$ (dashed) defined by (12) and (16). The shear-compression ratio is $g = 2.5$.

Remark 2. *If a beam is homogeneous on the whole domain* $[0, L]$*, by choosing* $A_c = A$ *and* $I_c = I$ *in the scaling* (4)*, one obtains* $\mathcal{A} = \mathcal{I} = 1$ *and* $\alpha = 1$*. For piecewise homogeneous beams, if the same scaling is used throughout the whole beam (by* e.g. *choosing* A_c *and* I_c *as the mean values of* A *and* I*),* α *takes different values in each subdomain and different bases of solutions* $\Psi^{\omega,\alpha}$ *should be used throughout the beam.*

Exponentially varying beams. Other simple solutions exist for beams whose profiles are exponentially varying at the same rate: $\mathcal{A}(x) = \mathcal{A}_0 e^{2\delta x}$ and $\mathcal{I}(x) = \mathcal{I}_0 e^{2\delta x}$, *e.g.* beams with rectangular cross-sections having a constant thickness and an exponentially varying width. Then, keeping the notation $\alpha = \mathcal{A}/\mathcal{I} = \mathcal{A}_0/\mathcal{I}_0$, the system (5) becomes:

$$\begin{cases} (u' - \theta)' + 2\delta(u' - \theta) + \omega^2 u = 0 \\ g\,(\theta'' + 2\delta\theta') + \alpha(u' - \theta) + \omega^2\theta = 0. \end{cases} \tag{14}$$

Looking for oscillating solutions $e^{\mathrm{i}kx}$ for both u and θ, the dispersion relation is found to be:

$$g\widehat{K}^2 - \omega^2(1 + g)\widehat{K} + \omega^2(\omega^2 - \alpha) = 0, \quad \text{with} \quad \widehat{K} = k^2 - 2\mathrm{i}\delta k. \tag{15}$$

This is exactly the equation (10) obtained for homogeneous beams, except that $K = k^2$ is replaced by $\widehat{K}$. The roots are K_+ and K_-, as given by (11), and the associated wavenumbers are:

$$\widehat{k}_1 = \mathrm{i}\delta + \sqrt{K_+ - \delta^2}, \quad \widehat{k}_2 = \mathrm{i}\delta - \sqrt{K_+ - \delta^2}, \quad \widehat{k}_3 = \mathrm{i}\delta + \sqrt{K_- - \delta^2}, \quad \widehat{k}_4 = \mathrm{i}\delta - \sqrt{K_- - \delta^2}. \tag{16}$$

Eventually, the basis of solutions of the system (14), parametrized by α and δ, is:

$$\Psi^{\omega,\alpha,\delta} = \left\{x \mapsto e^{\mathrm{i}\widehat{k}_m x}\right\}_{m=1..4} = \left\{x \mapsto e^{-\delta x} e^{\mathrm{i}s_m x\sqrt{(k_m)^2 - \delta^2}}\right\}_{m=1..4}, \quad s_m := (-1)^{m-1}. \tag{17}$$

This solution is also given by other authors [33, 36] with slightly different notations.

Other exact solutions. The paper by Yuan et al. [36] provides other closed-form solutions, for several "complex exponential" (*i.e.* exponential of polynomials) and polynomial profiles. These solutions are written in terms of hypergeometric functions. Exact solutions are also built by Sarkar and Ganguli [25] for geometrically homogeneous but materially graded beams. An inverse point of view is adopted: a polynomial solution (u, θ) that satisfies prescribed boundary conditions is chosen, and then one determines the polynomial profiles of material parameters that permit to recover this solution. Semi-analytical solutions are also available, *e.g.* Eisenberger [8] considers polynomial variations of $\mathcal{A}$ and $\mathcal{I}$ and expands the solution as a power series, whose coefficients are shown to satisfy recurrence relations, and Sohani and Eipakchi [29] propose a perturbation approach based on the WKB expansion to tackle the heterogeneity.

3. Enriched finite elements

In this section, we begin by briefly recalling the principles of the Finite Element Method (FEM) applied to the Timoshenko system (for further details, we refer to the textbooks [16, 9]). Then, we present an enrichment method dedicated to the construction of discrete approximation spaces adapted to specific problems, and use it to build Timoshenko-adapted spaces.

3.1. Weak formulation

The first step to apply the FEM is to write the weak formulation of the problem. First, let us recall some notations for the functional spaces used thereafter [9, App. B]. As usual, $L^2(0,L)$ denotes the space of square-integrable functions on $]0,L[$ and:

$$\begin{aligned} H^1(0,L) &:= \left\{ f \mid f \in L^2(0,L) \text{ and } f' \in L^2(0,L) \right\}, \\ H^1_{(0}(0,L) &:= \left\{ f \in H^1(0,L),\ f(0) = 0 \right\}, \\ H^1_0(0,L) &:= \left\{ f \in H^1(0,L),\ f(0) = 0 \text{ and } f(L) = 0 \right\}. \end{aligned} \tag{18}$$

Then, multiplying the two lines of the system (5) by two test functions v and ϕ, integrating by parts, summing the resulting equalities, one obtains the weak formulation of the Timoshenko problem (*i.e.* of the system (5) associated with a given set of BCs) as:

$$\begin{aligned} \text{Find } (u,\theta) \in \boldsymbol{\mathcal{V}} \text{ such that } \int_0^L \mathcal{A}(u'-\theta)(v'-\phi) + g\mathcal{I}\theta'\phi' - \omega^2(\mathcal{A}uv + \mathcal{I}\theta\phi) \\ = \int_0^L (qv + m\phi) + \Big[Nv + M\phi\Big]_0^L \quad \text{for all } (v,\phi) \in \boldsymbol{\mathcal{V}}_0, \end{aligned} \tag{19}$$

where the *space of kinematically admissible fields* $\boldsymbol{\mathcal{V}}$ is a subspace of $(H^1(0,L))^2$ that depends on the kinematic boundary conditions that are imposed on u or θ; $\boldsymbol{\mathcal{V}}_0$ is the associated linear space (corresponding to homogeneous kinematic BCs); and the boundary term $[Nv + M\phi]_0^L$ depends on all BCs. Some examples include:

- the *glued-glued beam*, for which (u,θ) vanishes at both extremities. In this case, $\boldsymbol{\mathcal{V}} = \boldsymbol{\mathcal{V}}_0 = (H^1_0(0,L))^2$, the boundary term vanishes and the motion is only due to the force density q or the moment density m.
- the *cantilever beam*, for which $(u,\theta)(0) = (0,0)$ and the shear force and bending moment are imposed at the right extremity: $N(L) = N_\star$ and $M(L) = M_\star$. In this case, the functional space is $\boldsymbol{\mathcal{V}} = \boldsymbol{\mathcal{V}}_0 = (H^1_{(0}(0,L))^2$, and the boundary contribution is:
$$\Big[Nv + M\phi\Big]_0^L = N_\star v(L) + M_\star \phi(L). \tag{20}$$
- the *glued-free beam* submitted to time-harmonic displacement with amplitude $u_\star$ at $x = 0$ (*i.e.* $u(0) = u_\star$ and $\theta(0) = 0$) and free at $x = L$ (*i.e.* $N(L) = 0$ and $M(L) = 0$). Then one has:
$$\boldsymbol{\mathcal{V}} = \{(u,\theta) \in H^1(0,L) \times H^1_{(0}(0,L),\ u(0) = u_\star\}, \qquad \boldsymbol{\mathcal{V}}_0 = (H^1_{(0}(0,L))^2, \tag{21}$$
and the boundary term entirely vanishes.

In the third example above, and more generally when non-homogeneous kinematic BCs are imposed, $\boldsymbol{\mathcal{V}}$ is an affine space, *i.e.* $\boldsymbol{\mathcal{V}} \neq \boldsymbol{\mathcal{V}}_0$. However, one easily comes back to the configuration $\boldsymbol{\mathcal{V}} = \boldsymbol{\mathcal{V}}_0$ by considering a *lifting* of a problem, *i.e.* by defining new unknowns $(u_\ell, \theta_\ell) := (u,\theta) - (\hat{u},\hat{\theta}) \in \boldsymbol{\mathcal{V}}_0$, where $(\hat{u},\hat{\theta})$ is an arbitrary element of $\boldsymbol{\mathcal{V}}$.

For instance, taking $(\hat{u},\hat{\theta}) = (\hat{u}_\star, 0)$, where $\hat{u}_\star$ is a chosen function of $H^1(0,L)$ such that $\hat{u}_\star(0) = u_\star$, the lifted counterpart of the glued-free beam problem (19)–(21) is:

$$\begin{aligned} \text{Find } (u_\ell,\theta_\ell) \in \boldsymbol{\mathcal{V}}_0 \text{ such that } \int_0^L \mathcal{A}(u_\ell'-\theta_\ell)(v'-\phi) + g\mathcal{I}\theta_\ell'\phi' - \omega^2(\mathcal{A}u_\ell v + \mathcal{I}\theta_\ell\phi) \\ = \int_0^L (qv + m\phi) - \int_0^L \mathcal{A}\Big(\hat{u}_\star'(v'-\phi) - \omega^2\hat{u}_\star v\Big) \quad \text{for all } (v,\phi) \in \boldsymbol{\mathcal{V}}_0, \end{aligned} \tag{22}$$

where $\boldsymbol{\mathcal{V}}_0$ is given by (21). Then the solution of the original problem is $(u,\theta) = (u_\ell + \hat{u}_\star, \theta_\ell)$.

Since such a lifting is always possible, it is assumed that $\boldsymbol{\mathcal{V}} = \boldsymbol{\mathcal{V}}_0$ in all the considered problems hereafter.

3.2. Finite element method

The finite element method belongs to the family of *Galerkin methods*, that rely on an approximation of the trial space $\mathcal{V}_0$ by a finite-dimension subspace $\mathcal{V}_{h,0} \subset \mathcal{V}_0$. In this work, the same approximation space is used for u and θ, and therefore we first look for a subspace $\mathcal{V}_h$ of $H^1(0, L)$, whose dimension is noted N_h, and then define $\boldsymbol{\mathcal{V}}_h = (\mathcal{V}_h)^2$ the corresponding space of couples (u_h, θ_h). The subspace $\boldsymbol{\mathcal{V}}_{h,0} = \boldsymbol{\mathcal{V}}_0 \cap \boldsymbol{\mathcal{V}}_h$ is finally built by removing the functions that does not satisfy the kinematic boundary conditions on u or θ from the basis of $\boldsymbol{\mathcal{V}}_h$.

In practice, this last step is performed at the end of the discretization process described now. First, the displacement and the rotation angle are approximated using the same basis $\{\varphi_j\}_{j=1..N_h}$ of $\mathcal{V}_h$, *i.e.* we look for approximations (u_h, θ_h) of (u, θ) as:

$$u_h = \sum_{j=1}^{N_h} u_j \varphi_j \qquad \text{and} \qquad \theta_h = \sum_{j=1}^{N_h} \theta_j \varphi_j. \tag{23}$$

By inserting these approximations into the weak formulation (19), and using the couples $(v, \phi) = (\varphi_i, 0)$ and $(v, \phi) = (0, \varphi_i)$ as test functions, one obtains the $2N_h \times 2N_h$ linear system:

$$(\boldsymbol{K} - \omega^2 \boldsymbol{M}) \cdot \boldsymbol{U} = \boldsymbol{F}, \tag{24}$$

where the vector $\boldsymbol{U}$ contains the discrete unknowns u_j and θ_j. In this work, we chose to dispose these values alternatively:

$$\boldsymbol{U} = [u_1,\ \theta_1, \dots,\ u_j,\ \theta_j, \dots u_{N_h}\ \theta_{N_h}]^{\mathrm{T}}, \quad \textit{i.e.} \quad U_{2j-1} = u_j \quad \text{and} \quad U_{2j} = \theta_j, \quad j = 1 \dots N_h, \tag{25}$$

so that the components of the stiffness matrix $\boldsymbol{K}$ are:

$$\begin{aligned} K_{2i-1,2j-1} &= \int_0^L \mathcal{A}\varphi_i'\varphi_j', \quad K_{2i-1,2j} = -\int_0^L \mathcal{A}\varphi_i'\varphi_j, \\ K_{2i,2j-1} &= -\int_0^L \mathcal{A}\varphi_i\varphi_j', \quad K_{2i,2j} = \int_0^L \mathcal{A}\varphi_i\varphi_j + g\mathcal{I}\varphi_i'\varphi_j', \end{aligned} \tag{26}$$

and those of the mass matrix $\boldsymbol{M}$ are:

$$M_{2i-1,2j-1} = \int_0^L \mathcal{A}\varphi_i\varphi_j, \qquad M_{2i,2j} = \int_0^L \mathcal{I}\varphi_i\varphi_j, \tag{27}$$

and $M_{2i-1,2j} = M_{2i,2j-1} = 0$. The right-hand-side vector $\boldsymbol{F}$ is decomposed into $\boldsymbol{F} = \boldsymbol{F}^{\mathrm{in}} + \boldsymbol{F}^{\mathrm{bc}}$, where $\boldsymbol{F}^{\mathrm{in}}$ contains the contribution of the force and moment densities:

$$F^{\mathrm{in}}_{2i-1} = \int_0^L q\varphi_i, \qquad F^{\mathrm{in}}_{2i} = \int_0^L m\varphi_i, \tag{28}$$

and $\boldsymbol{F}^{\mathrm{bc}}$ accounts for the boundary conditions on N or M. For instance, for glued-glued beams one has $\boldsymbol{F}^{\mathrm{bc}} = \boldsymbol{0}$, and for cantilever beams, using (20) one has $\boldsymbol{F}^{\mathrm{bc}} = \boldsymbol{F}^{\mathrm{bc,ct}}$ with:

$$F^{\mathrm{bc,ct}}_{2i-1} = N_\star \varphi_i(L), \qquad F^{\mathrm{bc,ct}}_{2i} = M_\star \varphi_i(L). \tag{29}$$

The steps described above only take into account the boundary conditions on N and M. The last step to adapt the system (24) to a given problem is to impose that u_h and θ_h satisfy the prescribed kinematic BCs. To this end, we remove from the approximation basis of each variable the functions φ_j that does not vanish at the extremity where these conditions are imposed (equivalently, the associated coefficients u_j and θ_j are set to 0 in (23)). The corresponding lines and columns are finally removed from the system (24).

The quality of the approximation obtained by solving this system depends on the interpolation properties of the chosen space $\mathcal{V}_h$, *i.e.* the minimal distance between the exact solution of the system and a function of $\boldsymbol{\mathcal{V}}_h$. For many applications, well-documented spaces of piecewise-polynomial functions [16, 9] offer very good performances. However, for some problems, including medium- or high-frequency vibration problems, polynomials need refined meshes and therefore high computational cost to catch the fast oscillations of the solution. The alternative we propose is to build enriched spaces by incorporating oscillating functions into the elementary bases, as presented now.

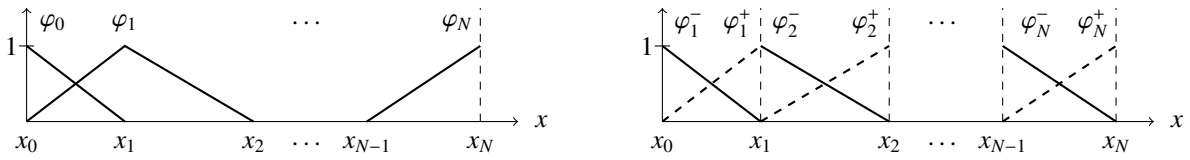

Figure 3: "Hat" (left) and "half-hat" (right) functions defined from a mesh $\{x_0,\ x_1,\ ...,\ x_N\}$.

3.3. Building enriched spaces using the "half-hat" partition of unity

To incorporate enrichment functions in an approximation space, we follow the partition of unity method introduced by Melenk and Babuška [20], which is adapted to the Timoshenko problem as follows. One must first define a partition of unity, *i.e.* a family of functions $\{\varphi_n\}_{n=0..N}$ that satisfies:

$$\sum_{n=0}^{N} \varphi_n(x) = 1, \quad \forall x \in [0, L].$$

Given another family of functions $\Psi = \{\psi^m\}_{m=1..N_m}$ that gathers functions that will be added in the approximation space and that we therefore call the *enrichment family*, one then builds an *enriched function space* $\mathcal{V}_h^\Psi$ as:

$$\mathcal{V}_h^\Psi = \text{span}\{\varphi_n^m\}_{n=0..N,\ m=0..N_m} \quad \text{with} \quad \begin{cases} \varphi_n^0 = \varphi_n, \\ \varphi_n^m = \varphi_n \psi^m. \end{cases} \tag{30}$$

A function $u_h \in \mathcal{V}_h^\Psi$ is defined by its $(N+1) \times (N_m+1)$ components u_n^m in the basis $\{\varphi_n^m\}$:

$$u_h = \sum_{n=0}^{N} \sum_{m=0}^{N_m} u_n^m \varphi_n^m. \tag{31}$$

The most commonly used PU is the family of "hat" functions, to which the notation φ_n will apply hereafter, defined from a mesh $\{0 = x_0,\ x_1,\ ...,\ x_N = L\}$ of $[0, L]$ as plotted in Figure 3. Indeed, these functions form a basis of the traditional FE space of piecewise-linear functions [9], and this choice allows to retain some convenient properties of this basis for the enriched space, notably the sparsity of stiffness and mass matrices [20, 31].

However, with such a PU the additional functions $\varphi_n^m = \varphi_n \psi^m$ are supported by two elements. To restrain their support to one element only, we proposed in a previous work [7] to support the enrichment using the "half-hat" PU represented in Figure 3. Since on the e-th element the couple $\{\varphi_e^-, \varphi_e^+\}$ forms a local partition of unity, one can work directly on the elementary basis and choose a specific enrichment family Ψ_e for each element. We additionally impose that the additional functions cancel at the end of each element, which simplifies the implementation of the resulting method and allows one to apply the static condensation procedure, as developed in Section 5.1 below.

For each enrichment function ψ_e^m in Ψ_e, two additional functions φ_e^{m-} and φ_e^{m+} are therefore added to the elementary basis. Written as functions of the normalized coordinate $\xi = (x - x_{e-1})/h_e \in [0, 1]$, where $h_e := x_e - x_{e-1}$ is the length of the e-th element, they read:

$$\varphi_e^{m-}(\xi) = (1-\xi)\left[\psi_e^m(x_{e-1} + h_e\xi) - \psi_e^m(x_{e-1})\right], \quad \varphi_e^{m+}(\xi) = \xi\left[\psi_e^m(x_{e-1} + h_e\xi) - \psi_e^m(x_e)\right]. \tag{32}$$

Remark 3. *When the space generated by the enrichment family is invariant by shifting the origin of the x-axis (typically, when the family embeds only exponential functions* e.g. $\psi_e^m(x) = \exp(\mathrm{i}k_m x)$*), it is convenient to use the definitions:*

$$\varphi_e^{m-}(\xi) = (1-\xi)\left[\psi_e^m(h_e\xi) - \psi_e^m(0)\right], \quad \varphi_e^{m+}(\xi) = \xi\left[\psi_e^m(h_e(\xi-1)) - \psi_e^m(0)\right], \tag{33}$$

instead of (32)*, in particular for implementation easiness. These alternative definitions are used hereafter.*

Then, we look for approximations (u_h, θ_h) as linear combinations of "hat" functions (to ensure that these approximations belongs to $H^1(0, L)$, see [7]) and those inner additional functions. Hereafter, we use the same number N_m of enrichment functions for all elements, and such a combination is therefore written:

$$u_h = \sum_{n=0}^{N} u_n^0 \varphi_n^0 + \sum_{e=1}^{N} \sum_{m=1}^{N_m} \left[u_e^{m+} \varphi_e^{m+} + u_e^{m-} \varphi_e^{m-} \right]. \tag{34}$$

In the sum (34), the distinction is made between the *nodal values* u_n^0 associated with the "hat" functions, and the *inner values* $u_e^{m\pm}$ associated with the additional inner functions. The approximation space embedding all these combinations is:

$$\mathcal{P}_{1,2m} = \text{span}\left\{ \left\{\varphi_n^0\right\}_{n=0..N} \bigcup \{\varphi_e^{m+}, \varphi_e^{m-}\}_{e=1..N,\ m=1..N_m} \right\}, \tag{35}$$

whose dimension is $\dim \mathcal{P}_{1,2m} = (N+1) + 2N \times N_m$.

Finally, specifying kinematic boundary conditions corresponding to a given problem is done by fixing only the boundary values $u_0^0 = u_h(0)$ and $u_N^0 = u_h(L)$, and similarly for θ_h, while boundary conditions on N and M are accounted for in the weak formulation (19).

Remark 4. *Note that the notation was slightly modified compared to our previous work [7]: the "half-hat" functions $\varphi_e^{\pm}$ and elementary functions $\varphi_e^{m\pm}$ are now associated with a given element (thus the subscript $\cdot_e$); and the + and − exponents now indicate the sign of the slope of the functions $\varphi_e^{\pm}$.*

3.4. Enriched spaces dedicated to Timoshenko beams

To conclude this section, we present the spaces obtained by combining the bases of solutions for homogeneous or exponential beams given in Section (2.2) and the enrichment procedure described above. We also briefly present spaces that will be used as reference in the numerical illustrations.

Timoshenko-enriched spaces. The first enriched space we consider, noted $\mathcal{P}_{1,8}^{\omega,\alpha}$, is obtained from the solutions $\Psi^{\omega,\alpha}$ corresponding with a homogeneous beam, given by (13). For arbitrary heterogeneous beams, the function $\alpha = \mathcal{A}/\mathcal{I}$ is used to define enrichements to each elementary basis: the e-th basis is enriched with the family Ψ^{ω,α_e}, where $\alpha_e := \alpha((x_{e-1} + x_e)/2)$ is the value of α at the middle point of the e-th element. Following (33), the eight additional inner functions are:

$$\varphi_e^{m-}(\xi) = (1-\xi)\left[e^{\mathrm{i}k_m h_e \xi} - 1\right] \quad \text{and} \quad \varphi_e^{m+}(\xi) = \xi\left[e^{\mathrm{i}k_m h_e (\xi-1)} - 1\right] \quad (m = 1\,..\,4), \tag{36}$$

where the wavenumbers k_m given by (12) depend on α_e. These functions are represented in Figure 4. The enriched space then embeds the exact solution for a piecewise-homogeneous or "step" beam, free from linear excitations.

We then introduce the space $\mathcal{P}_{1,8}^{\omega,\alpha,\delta}$, whose elementary bases are enriched with the solutions $\Psi^{\omega,\alpha_e,\delta_e}$ corresponding to exponential beams, defined by (17). For each element, the parameters α_e and δ_e are the values of α and $\delta := \mathcal{A}'/2\mathcal{A}$ at the middle of the element. The additional inner functions are defined similarly to (36), but with the wavenumbers $\{k_m\}_{m=1..4}$ replaced by their counterparts $\{\widehat{k_m}\}_{m=1..4}$ defined by (16).

In the particular case of beams with constant thickness, $\alpha = \mathcal{A}/\mathcal{I}$ is constant and therefore all elementary bases are identical for the sapce $\mathcal{P}_{1,8}^{\omega,\alpha}$: it is then a *globally* enriched space and does not depend on the inhomogeneity of the beam. In this case, using the second space $\mathcal{P}_{1,8}^{\omega,\alpha,\delta}$, which is still *locally* enriched when δ is inhomogeneous, is a first way to take the width variations into account.

Remark 5. *The spaces $\mathcal{P}_{1,8}^{\omega,\alpha}$ and $\mathcal{P}_{1,8}^{\omega,\alpha,\delta}$ are the counterparts for Timoshenko beams of the spaces $\mathcal{P}_{1,4}^{k}$ and $\mathcal{P}_{1,4}^{k,\delta}$ built in [7] from time-harmonic solutions corresponding to homogeneous and exponentially varying bars.*

For completeness, some other enriched spaces that produced similar results on the upcoming test-cases are presented in Appendix A.

Reference spaces. To assert the efficiency of the enriched spaces, we will compare their performance with more classical spaces. As a reference space, we chose the space $\mathcal{P}_9$ of piecewise ninth-order polynomials, whose implementation is identical to the one of the enriched spaces $\mathcal{P}^{\omega,\alpha}_{1,8}$ and $\mathcal{P}^{\omega,\alpha,\delta}_{1,8}$ since it also features two nodal and eight inner functions per elementary basis. Several elementary bases exist for this space, among them are the hierarchical basis of Lobatto polynomials (often implicitly associated with the so-called p or hp-FEM [16, Sect. 4.7]) and the "spectral" basis of Lagrange polynomials with interpolation nodes taken as the Gauss-Lobatto-Legendre points of the reference element [18, 30]. These two bases were compared by Sprague and Geers [30], and produced nearly identical results in terms of accuracy. Since the main advantage of spectral bases, namely the diagonal mass matrices they produce, is irrelevant for time-harmonic problems, we use a hierarchical basis for simplicity, represented in Figure 4.

Finally, to complete the comparison, we will also look at the performance of a "naively" sine-enriched space, where the simplest family of oscillating functions $\Psi^\omega := \{x \mapsto e^{\pm \mathrm{i}\omega x}\}$ is used to enrich each elementary basis. To maintain eight inner functions as in the other considered bases, Lobatto polynomials up to the fifth degree are also added to obtain a polynomial-enriched space denoted by $\mathcal{P}^{\omega}_{5,4}$, whose elementary basis is represented in Figure 4.

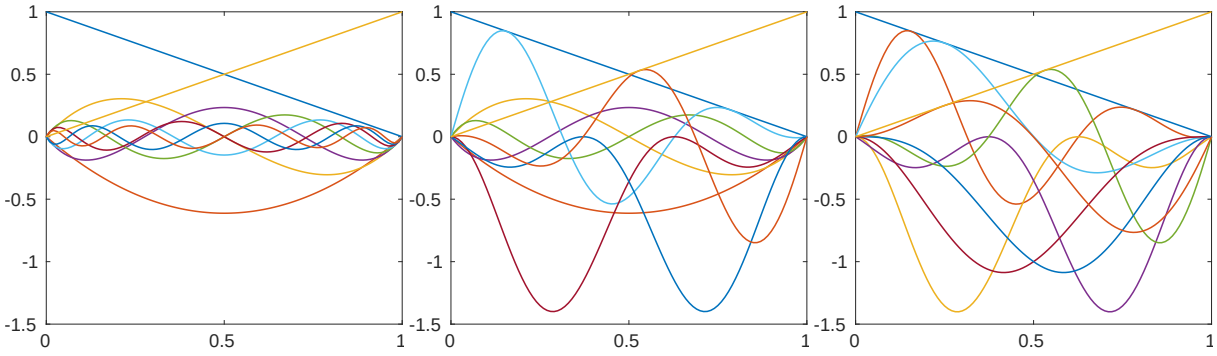

Figure 4: Elementary basis functions on an element of length $h = 1$. From left to right, hierarchical basis of Lobatto polynomials (space $\mathcal{P}_9$); sine-enriched basis for $\omega = 10$ (space $\mathcal{P}^{\omega}_{5,4}$); and Timoshenko-enriched basis for $\omega = 10$ and $\alpha = 1$ (space $\mathcal{P}^{\omega,\alpha}_{1,8}$).

4. A new formulation based on a local rescaling

For arbitrarily varying profiles $\mathcal{A}$, $\mathcal{I}$, the enrichment functions corresponding to homogeneous or exponentially varying beams account only partially for the geometry. To improve again the efficiency of the enriched method, we therefore propose to incorporate geometrical information into the problem unknowns before the discretization.

4.1. Change of unknowns in the Timoshenko system

Let us define the variable coefficients

$$d = \sqrt{\mathcal{A}} \quad \text{and} \quad a = \sqrt{\mathcal{I}}, \tag{37}$$

and new unknowns $(\tilde{u}, \tilde{\theta})$ obtained by the local (*i.e.* x-dependent) rescaling:

$$u = \frac{\tilde{u}}{d}, \qquad \theta = \frac{\tilde{\theta}}{a}. \tag{38}$$

This change of unknowns is inspired by a similar rescaling for Webster's equation $(\mathcal{A}u')' + k^2\mathcal{A}u + f = 0$, which models the longitudinal motion of beams [7], or low-frequency acoustic propagation in waveguides [24]. Indeed, when $\mathcal{A}$ is sufficiently regular, one has:

$$(\mathcal{A}u')' + k^2\mathcal{A}u + f = 0 \quad \Longleftrightarrow \quad \tilde{u}'' + \left(k^2 - \frac{d''}{d}\right)\tilde{u} + \frac{f}{d} = 0, \tag{39}$$

with $u = \tilde{u}/d$ and $d = \sqrt{\mathcal{A}}$, *i.e.* Webster's equation can be converted into a Helmholtz equation with variable wavenumber.

Similarly, introducing the rescaling (38) into the Timoshenko system (5) leads to:

$$\begin{cases} \left(d\tilde{u}' - d'\tilde{u} - \dfrac{d^2}{a}\tilde{\theta}\right)' + \omega^2 d\tilde{u} + q = 0 \\ g\left(a\tilde{\theta}' - a'\tilde{\theta}\right)' + \left(d\tilde{u}' - d'\tilde{u} - \dfrac{d^2}{a}\tilde{\theta}\right) + \omega^2 a\tilde{\theta} + m = 0. \end{cases} \tag{40}$$

Equivalently, expanding (40) and dividing the two lines by d and a, respectively, one obtains:

$$\begin{cases} \tilde{u}'' + \left(\omega^2 - \dfrac{d''}{d}\right)\tilde{u} = \dfrac{da\tilde{\theta}' + (2d'a - da')\tilde{\theta}}{a^2} - \dfrac{q}{d} \\ g\tilde{\theta}'' + \left(\omega^2 - \dfrac{d^2}{a^2} - g\dfrac{a''}{a}\right)\tilde{\theta} = -\dfrac{d\tilde{u}' - d'\tilde{u}}{a} - \dfrac{m}{a}. \end{cases} \tag{41}$$

The system (41) models two coupled harmonic oscillators, where the variable geometric parameters d and a intervene in the wavenumbers and the coupling terms, but not in the second-order terms in $\tilde{u}$ and $\tilde{\theta}$. We therefore expect $\tilde{u}$ and $\tilde{\theta}$ to be less affected by the inhomogeneity than the original solutions (u, θ), and therefore better approximated by oscillating enrichment functions corresponding to homogeneous beams. Of note, this is the case for exponentially varying beams with $\mathcal{A} = \mathcal{I}$: the solutions given by (17) are written $u = \tilde{u}/\sqrt{\mathcal{A}}$ where $\tilde{u}$ is a purely oscillating function.

4.2. Discretization

The weak formulation associated with the system (40) is:

$$\begin{aligned} \text{Find } (\tilde{u}, \tilde{\theta}) \in \widetilde{\boldsymbol{\mathcal{V}}} \text{ such that } \int_0^L \left(d\tilde{u}' - d'\tilde{u} - \frac{d^2}{a}\tilde{\theta}\right)(v' - \phi) + \int_0^L g\left(a\tilde{\theta}' - a'\tilde{\theta}\right)\phi' - \omega^2(duv + a\tilde{\theta}\phi) \\ = \int_0^L (qv + m\phi) + \Big[Nv + M\phi\Big]_0^L \quad \text{for all } (v, \phi) \in \boldsymbol{\mathcal{V}}_0, \end{aligned} \tag{42}$$

where we still note (v, ϕ) the test functions, and $\widetilde{\boldsymbol{\mathcal{V}}}$ is obtained by modifying the non-homogeneous kinematic boundary conditions embedded in the definition of $\boldsymbol{\mathcal{V}}$ accordingly with the change of unknowns (38). The associated linear space is $\widetilde{\boldsymbol{\mathcal{V}}}_0 = \boldsymbol{\mathcal{V}}_0$, so that, up to a lifting, the problem (42) may be also written using only $\boldsymbol{\mathcal{V}}_0$.

After discretization, the associated finite element system is:

$$(\widetilde{\boldsymbol{K}} - \widetilde{\boldsymbol{D}} - \omega^2\widetilde{\boldsymbol{M}}) \cdot \widetilde{\boldsymbol{U}} = \boldsymbol{F}, \tag{43}$$

where the components of the stiffness and mass matrices $\widetilde{\boldsymbol{K}}$ and $\widetilde{\boldsymbol{M}}$ have similar expressions than those of $\boldsymbol{K}$ and $\boldsymbol{M}$ defined by (26-27), with $\mathcal{A}$ and $\mathcal{I}$ replaced respectively by d and a, except for the components $\{\widetilde{K}_{2i,2j}\}_{i,j=1..N_h}$ where $\mathcal{A}$ is replaced by d^2/a instead. The matrix $\widetilde{\boldsymbol{D}}$ embeds the contributions of the derivatives d' and a' arising in (42) after the change of unknowns:

$$\begin{aligned} \widetilde{D}_{2i-1,2j-1} &= \int_0^L d'\varphi_i'\varphi_j, & \widetilde{D}_{2i-1,2j} &= -\int_0^L d'\varphi_i\varphi_j, \\ \widetilde{D}_{2i,2j-1} &= 0, & \widetilde{D}_{2i,2j} &= \int_0^L ga'\varphi_i'\varphi_j, \end{aligned} \tag{44}$$

and the right-hand side vector $\boldsymbol{F}$ is left unchanged and is defined by (29). Contrary to the system (24), the system (43) is not symmetric, due to the contribution of $\widetilde{\boldsymbol{D}}$.

4.3. Enriched spaces

Finally, approximations $(\tilde{u}_h, \tilde{\theta}_h)$ of $(\tilde{u}, \tilde{\theta})$ will be sought in the spaces $\mathcal{P}_9$, $\mathcal{P}^{\omega}_{5,4}$ and $\mathcal{P}^{\omega,\alpha}_{1,8}$ defined in Section 3.4. The corresponding spaces of solutions (u, θ) embedding the local rescaling are denoted by $\widetilde{\mathcal{P}}$, *e.g.* :

$$\widetilde{\mathcal{P}}_9 := \left\{ \left(\frac{\tilde{u}_h}{d}, \frac{\tilde{\theta}_h}{a} \right),\ (\tilde{u}_h, \tilde{\theta}_h) \in (\mathcal{P}_9)^2 \right\},\ d = \sqrt{\mathcal{A}},\ a = \sqrt{I}. \tag{45}$$

We define similary $\widetilde{\mathcal{P}}^{\omega}_{5,4}$ and $\widetilde{\mathcal{P}}^{\omega,\alpha}_{1,8}$: in the case where d and a are constant, the system (40) degenerates as expected into the α-dependent system (9) with $\alpha = d^2/a^2$, so using the associated solutions is still relevant for the modified formulation. On the contrary, there is no physically-based counterpart to the space $\mathcal{P}^{\omega,\alpha,\delta}_{1,8}$ and attempts to define a similar enriched space were not conclusive, see Appendix A.

5. Numerical validation and illustrations

This part first presents some general peculiarities of the implementation of the enriched FEM. Then, we explain how we validated the method by comparing its performances with the reference ninth-order FEM on test-cases with analytical solutions. Finally, we present and discuss the results obtained by simulating the vibrations of four beams with various heterogeneous geometries.

The result displayed below were obtained with an implementation of the method in a standard Matlab framework.

5.1. Implementation choices

Numerical integration. To compute the matrices' components (26,27,44), we used a classical Gauss quadrature [9, Sect. 8] and the following procedure to ensure that the integration of oscillatory basis functions remains accurate even for large elements supporting several wavelengths.

We first introduce a reference dimensionless wavelength independent of the considered beam:

$$\lambda := 2\pi/\omega, \tag{46}$$

which is the smallest wavelength in homogeneous and exponentially varying beams at the high-frequency limit, as discussed in Section 2.2. Then, each element is divided into $N_{\text{se}} := \lceil h/2\lambda \rceil$ subelements of equal lengths, where $h = \max_{n=1\ldots N} h_n$ and $\lceil \cdot \rceil$ denotes the ceiling function so that $\lceil x \rceil - 1 < x \leq \lceil x \rceil$ for any $x \in \mathbb{R}$. Then, 10 Legendre-Gauss points are used in each subelement to compute its contribution to the total integral. In this way, each subelement covers at most half of a wavelength λ, and there are at least 20 integration points per wavelength.

Static condensation. Since all the elementary bases presented above feature two nodal and eight inner basis functions, the same *static condensation* (SC) procedure can be applied to the linear systems (24) and (43). This procedure is described in details *e.g.* in the monograph by Ihlenburg [16, Sec. 4.7.3], and is also called *dynamic reduction* by some authors [28, Sect. 2.3]. In short, it first intervenes in the matrices assembly process: the inner values are expressed in terms of the nodal values by inverting each 8×8 inner elementary matrix. Then only the nodal values are retained as unknowns, and the global matrix to be inverted is therefore much smaller than the initial one, *e.g.* $2N \times 2N$ instead of $10N \times 10N$ for a cantilever beam. This matrix is also better conditioned than the original one, while only the small 8×8 elementary matrices inverted at the condensation step suffer from bad conditioning. Finally a post-processing operation (the decondensation) is needed to retrieve the inner values from the node values.

5.2. Validation of the method

First, the implementation of the polynomial and enriched FE bases are validated by comparison with analytical solutions. The accuracy of a FE solution (u_h, θ_h) compared to the exact solution (u, θ) is measured by the relative error $E_{\mathcal{L}}$ defined by:

$$E_{\mathcal{L}}(u_h, \theta_h) := \|(u_h - u, \theta_h - \theta)\|_{\mathcal{L}} \ / \ \|(u, \theta)\|_{\mathcal{L}}, \tag{47}$$

where we define the Lagrangian-based norm $\|\cdot\|_{\mathcal{L}}$ by:

$$\|(u,\theta)\|_{\mathcal{L}} = (-\mathcal{L}(u,\theta))^{1/2} = \left(\int_0^L \mathcal{A}(u'-\theta)^2 + g\mathcal{I}(\theta')^2 + \omega^2(\mathcal{A}u^2 + \mathcal{I}\theta^2)\right)^{1/2}, \tag{48}$$

where $\mathcal{L}(u,\theta)$ is the Lagrangian of the state (u,θ), *i.e.* the difference between the associated kinetic and elastic energies. This norm was also chosen for its similarity with the weighted H^1-norm $\|u\|^2_{H^1,k} := \|u'\|^2_{L^2} + k^2\|u\|^2_{L^2}$ that appears in the analysis of problems modeled by the Helmholtz equation $-u'' - k^2u = f$, to balance the weight of a function u and its derivatives for oscillating solutions. In practice, a discrete counterpart of the integral (48) is computed using the middle-point method and a very thin dedicated mesh (1001 elements) independent of the FE meshes.

The tests are performed on cantilever beams, glued at $x = 0$, *i.e.* $(u,\theta)(0) = (0,0)$, and with imposed transverse force and bending moment at $x = L$: either $(N,M)(L) = (1,0)$ or $(N,M) = (0,0)$ (free extremity) when the loading is provided by a linear density of forces q. We study the accuracy of the FE solutions for several *resolutions* λ/h, where $h = \max_n h_n$ is the largest element length and $\lambda = 2\pi/\omega$ is the reference wavelength as above. The resolution is an indicator of the *number of elements per smallest wavelength*, that is a relevant criterion to compare several FE spaces having the same number of basis functions per element when solving time-harmonic problems. The variation of the resolution is performed in two ways:

- First, the frequency ω is fixed and the error is computed for several regular meshes, *i.e.* for different element length h. For piecewise-smooth profiles $(\mathcal{A},\mathcal{I})$, the exact solution is also piecewise-smooth, and therefore the error (47) should decrease like h^9 as the mesh step h decreases when using the space $\mathcal{P}_9$, according to the classical theory for polynomial finite elements [16, 9] and provided that nodes are placed at the singularities of the profiles or their derivatives. Based on the results we previously proved for similar enriched spaces [7], we also expect the errors obtained with the enriched spaces $(\mathcal{P}^{\omega}_{5,4}, \mathcal{P}^{\omega,\alpha}_{1,8}, ...)$ to decrease with the same rate.
- Then, we fix the mesh and increase the frequency ω. In this way, we will observe the frequency-dependent peculiarities of the enriched spaces. Indeed, the accuracy obtained with polynomial spaces depends mainly on the resolution λ/h, with a pollution error increasing with the frequency [16, Sect. 4.6]. On the contrary, the accuracy of enriched space is expected to be more stable thanks to the oscillatory enrichment functions determined from the frequency of each problem.

5.2.1. Homogeneous beams

For homogeneous beams, we do not display simulation results for brevity and refer instead to the similar results displayed below for an exponentially varying beam, but we checked that the following key properties are verified:

- The Timoshenko-enriched space $\mathcal{P}^{\omega,\alpha}_{1,8}$ embeds the analytical solution, and therefore produces errors close to machine precision.
- The other spaces ($\mathcal{P}_9$ and $\mathcal{P}_{5,4}$) produced errors that decrease with the same $O(h^9)$ rate at fixed frequency.

Moreover, the initial and modified formulations are identical, thus the effect of the local rescaling cannot be observed.

5.2.2. Exponentially varying beams

We now present in details the tests performed on an exponentially varying beam of length $L = 10$, whose profiles are:

$$\mathcal{A}(x) = \mathcal{I}(x) = e^{2\delta x}, \tag{49}$$

with δ chosen such that $\mathcal{A}(L) = 1/8$. For these profiles, the space $\mathcal{P}^{\omega,\alpha}_{1,8}$ does not contain the exact solution for free vibrations (17), but its "exponentially" enriched companion $\mathcal{P}^{\omega,\alpha,\delta}_{1,8}$ does. Moreover, the initial and modified formulations differ. Both the effects of the various enrichments and of the modified formulation can therefore be observed.

Point-like loading. We first consider a cantilever beam whose motion is only due to a time-harmonic transverse force applied at its right extremity, with amplitude $N(L) = 1$. In this case the exact solution is a combination of the free vibrations solutions given by (17).

In Figure 5 are plotted the displacement and rotation fields (u, θ) obtained with the various enriched spaces at medium frequency $\omega = 5$ and with a coarse mesh made of only $N = 2$ elements, so that the resolution is $\lambda/h \approx 1/4$ (one element for four wavelengths). We already observe qualitatively that, in this case, the sine-enriched space $\mathcal{P}^{\omega}_{5,4}$ outperforms the polynomial space $\mathcal{P}_9$ in the approximation of the displacement u (*i.e.* replacing four polynomials by oscillating functions already improves the quality of the results) and is outperformed by the spaces enriched by Timoshenko solutions, which are the only ones able to capture the oscillations of the rotation θ.

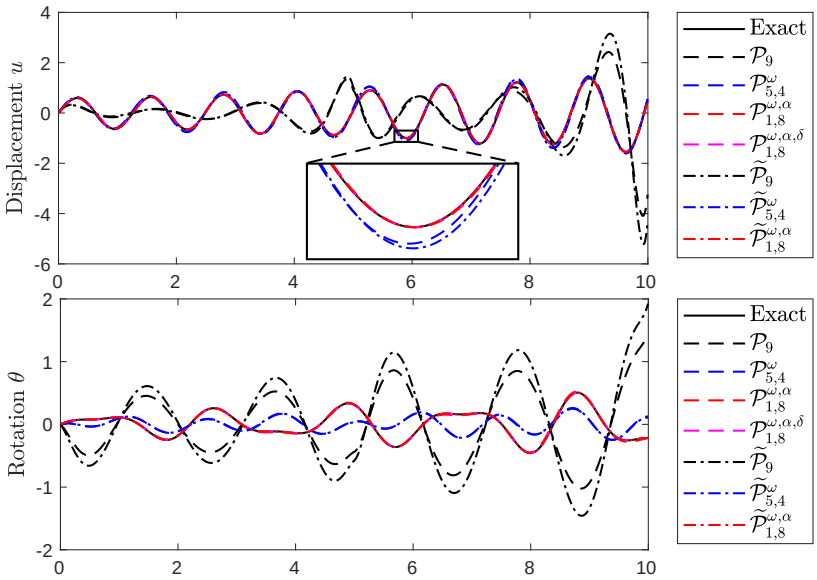

Figure 5: Exact and approached solutions u (top) and θ (bottom) for a cantilever beam with exponential profiles, for a circular frequency $\omega = 5$ and $N = 2$ elements. The Timoshenko-enriched solutions (red and pink) are superposed with the exact one (solid black).

Then, the relative errors obtained at the same fixed frequency $\omega = 5$ with several meshes are plotted in the left panel of Figure 6. Additional observations may be made:

- For coarse meshes, the exponential-enriched space $\mathcal{P}^{\omega,\alpha,\delta}_{1,8}$ that embeds the analytical solution reaches the machine precision (see below for refined meshes).
- In the convergence regime, all the other curves follow the expected $O(h^9)$ rate.
- The local rescaling does not affect the precision obtained with the polynomial space $\mathcal{P}_9$ and the sine-enriched space $\mathcal{P}^{\omega}_{5,4}$. On the other hand, it improves drastically (by several orders of magnitude) the precision obtained with $\mathcal{P}^{\omega,\alpha}_{1,8}$ (as expected in this particular case, because the amplitude factor $e^{-\delta x}$ of the solution is exactly embedded in the local rescaling).
- For each enriched spaces, there is a threshold above which the conditioning of the discrete system obtained with the enriched spaces penalizes the solution and the error begins to grow (see the discussion below). However, this threshold appears for small relative errors (lower than 10^{-8} for all the spaces in this example), and very acceptable errors can be obtained by choosing a medium-sized mesh. For instance, fixing $h = \lambda$ leads to relative errors varying between 10^{-4} ($\mathcal{P}_9$ and $\widetilde{\mathcal{P}}_9$) to 10^{-10} ($\widetilde{\mathcal{P}}^{\omega,\alpha}_{1,8}$).

In the right panel of Figure 6, we represented the errors obtained with a fixed mesh size $h = 1$ and increasing frequencies. For this test-case, the error evolution depends on the FE space. The errors associated with polynomial solutions increase regularly with ω as ω^9 (*i.e.* as $(h/\lambda)^9$ as expected), until they reach a plateau. On the contrary,

errors associated with enriched solutions (i) increase as $\omega \to 0$ (*i.e.* as the resolution increases) due again to bad conditioning, (ii) reach a minimum value for medium resolution and frequency and (iii) increase slower than ω^9 and finally seem to reach a plateau at low error levels. The local rescaling has a much more remarkable and frequency-dependent effect that leads to a high gain for high frequencies.

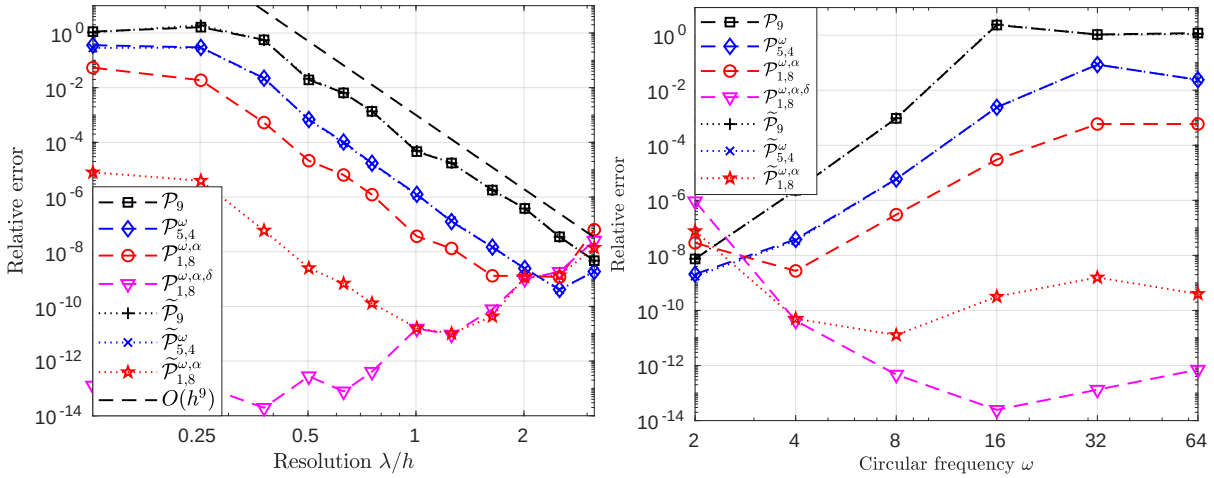

Figure 6: Relative errors for a cantilever beam with exponential profiles and $g = 2.5$. Left: the frequency is fixed to $\omega = 5$, and the resolution λ/h increases as the mesh is refined from 1 to 25 elements. Right: the mesh is fixed to $N = 10$ elements of length $h = 1$, and the frequency increases.

Distributed loading. As a second validation test, we consider the same exponentially varying cantilever beam, free at the right extremity, *i.e.* $(N, M)(L) = (0, 0)$, but submitted to a distributed loading. A linear density of forces with amplitude q_{P} corresponding to a particular solution $(u_{\text{P}}, \theta_{\text{P}})$ with $u_{\text{P}}(x) = (x/L)^2$ and linear θ_{P} is designed (see Appendix B for details), so that the exact solution is $(u, \theta) = (u_{\text{P}}, \theta_{\text{P}}) + (u_{\text{H}}, \theta_{\text{H}})$, where the "homogeneous" part $(u_{\text{H}}, \theta_{\text{H}})$ satisfies the system (14) and therefore is a combination of the free vibration solutions (17). This example is chosen so that none of the FE spaces contains the full solution: $\mathcal{P}_9$ and $\mathcal{P}^{\omega}_{5,4}$ contain the particular solution but not the homogeneous part, and $\mathcal{P}^{\omega,\alpha,\delta}_{1,8}$ contains the homogeneous part but not the particular solution.

Remark 6. *For this particular case, it would be easy to build a tenth-order space $\mathcal{P}^{\omega,\alpha,\delta}_{2,8}$ by adding an additional second-order polynomial shape function to the elementary bases of $\mathcal{P}^{\omega,\alpha,\delta}_{1,8}$, and therefore recover a space that contains the exact solution. More generally, when a particular solution is known exactly or approximately, higher-order FE spaces can be designed by incorporating relevant additional shape functions to the bases of existing spaces, either polynomials or other functions, using the half-hat PU.*

This solution (u, θ) is plotted in figure 7 for $\omega = 5$, along with the approximations obtained with the various spaces and for $N = 3$ elements. Again, for this configuration the enriched spaces clearly outperforms the polynomial space, especially for the approximation of the rotation θ. In figure 8, contrarily to the previous example, we observe that all the enriched spaces present similar performances, due to the additional force density. The local rescaling, which was designed by studying the Timoshenko system without source terms, always provides a slight error decrease.

Conditioning and static condensation. Finally, to better understand the conditioning effects, we plotted in Figure 9 the conditioning number of the matrices $\boldsymbol{K} - \omega^2 \boldsymbol{M}$ (for the original formulation) and $\widetilde{\boldsymbol{K}} - \widetilde{\boldsymbol{D}} - \omega^2 \widetilde{\boldsymbol{M}}$ (for the modified formulation) for the frequency $\omega = 5$ and the various meshes used in the two examples above (left panels of figures 6 and 8). On the left panel are plotted the average conditioning numbers of the 8×8 inner elementary matrices that gather the contributions of the inner functions for each element. As the definition of the elementary polynomial basis does not depend on the element size, the conditioning of the resulting matrices is almost insensitive to the resolution. On the contrary, the inner functions $\varphi_e^{m\pm}$ incorporated in the enriched bases become nearly linearly dependent as the resolution increases, and the conditioning number of the matrices explodes. This bad conditioning is reflected on the

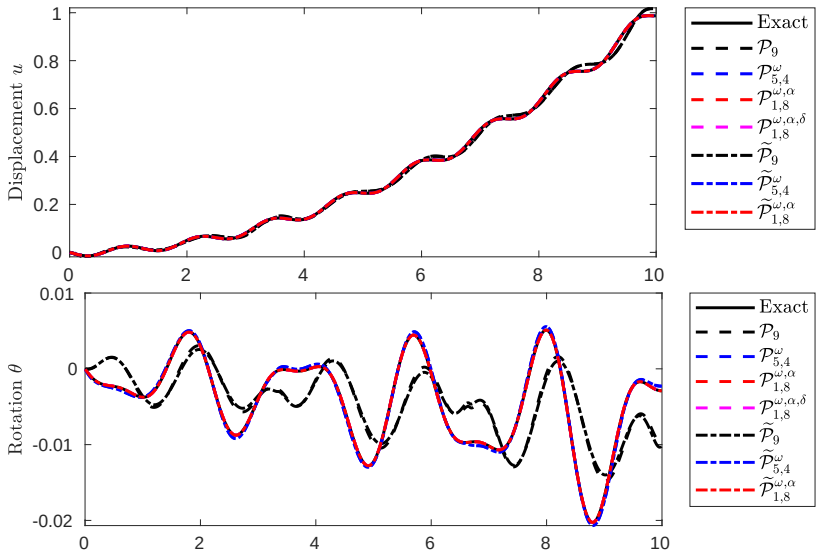

Figure 7: Exact and approached solutions u (top) and θ (bottom) for a cantilever beam with exponential profiles submitted to a distributed loading $q \neq 0$, for a circular frequency $\omega = 5$ and $N = 3$ elements. The Timoshenko-enriched solutions (red and pink) are superposed with the exact one (solid black).

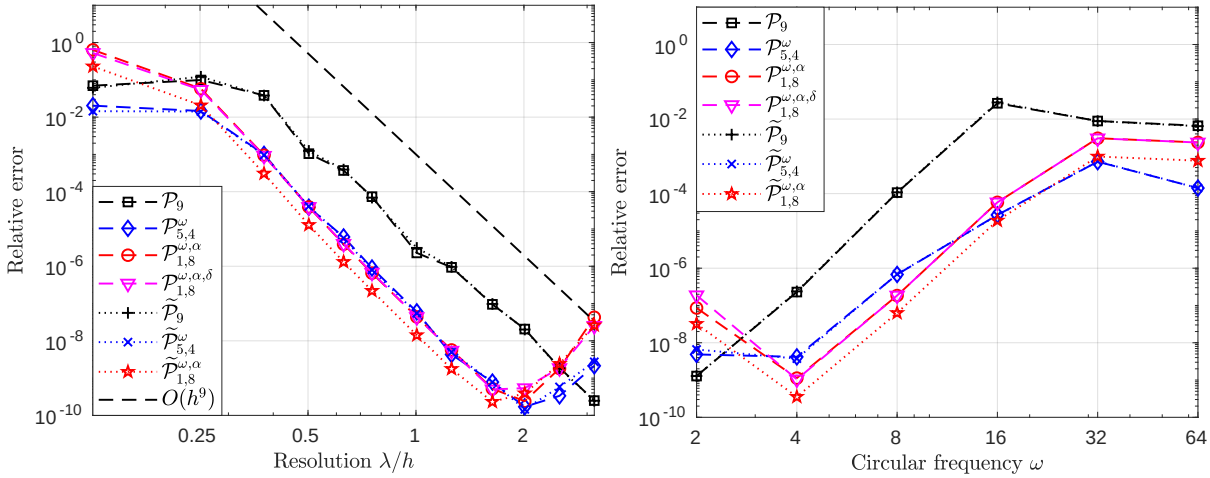

Figure 8: Relative errors for a cantilever beam with exponential profiles and $g = 2.5$, submitted to a distributed loading $q \neq 0$. Left: the frequency is fixed to $\omega = 5$, and the resolution λ/h increases as the mesh is refined from 1 to 25 elements. Right: the mesh is fixed to $N = 10$ elements of length $h = 1$, and the frequency increases.

global matrices (middle panel) and penalizes the accuracy of the solution for thin meshes ($h < \lambda$), as noticed above in Figures 6 and 8.

This bad conditioning is partially addressed by applying the static condensation method presented in Section 5.1: the condensed global matrices are not only smaller, but also well conditioned for all FE bases, as seen in the right panel of Figure 9. However, in this case the bad conditioning of elementary matrices still affects the accuracy of the solution, and results nearly identical to those of Figures 6 and 8 (not plotted for brevity) were obtained with the equivalent condensed system. Since the systems we solve are sufficiently small-sized to be solved rapidly without condensation, we therefore use the full uncondensed matrices in the upcoming examples for simplicity.

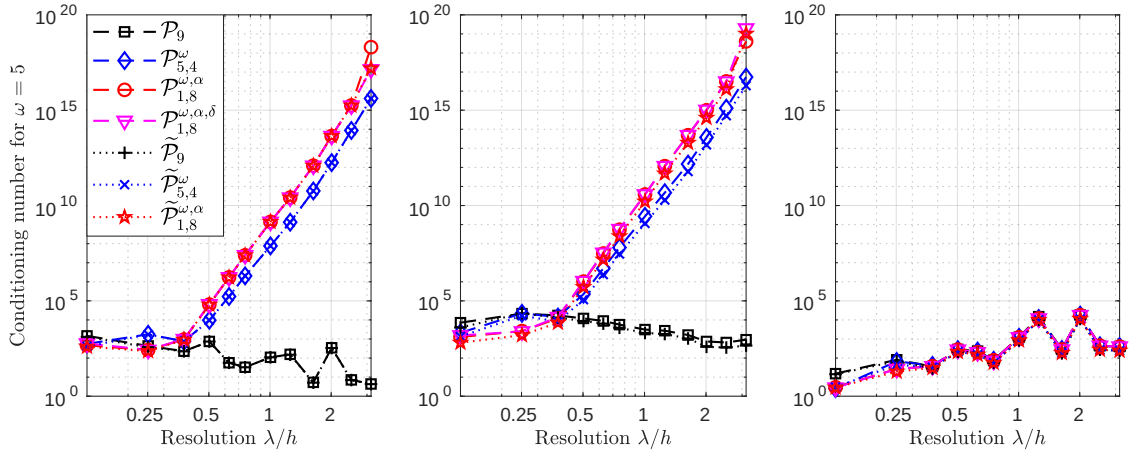

Figure 9: Conditioning numbers of the FE matrices corresponding to the results of Figure 6 obtained for an exponentially varying beam, for fixed frequency $\omega = 5$ and decreasing meshsize. Left: elementary 8×8 matrices corresponding to inner shape functions (the conditioning number is averaged over all the elements). Middle: matrices of the systems (24) and (43), without condensation. Right: condensed matrices.

5.3. Examples on heterogeneous beams

To show the efficiency of our method to handle the inhomogeneity of the beam, we now present the results obtained for four cantilever beams with boundary conditions $(u, \theta)(0) = (0, 0)$ and $(N, M)(L) = (1, 0)$, featuring various geometries for which no analytical solution is available. These test-cases are ordered by increasing complexity of the inhomogeneity: we study successively

1. a beam with constant thickness and quadratically varying width (so that $\mathcal{A} = \mathcal{I}$),
2. a conical beam with circular cross-section and linearly decreasing radius (so that $\mathcal{A} \neq \mathcal{I}$ but the profiles are still smoothly and simultaneously decreasing),
3. a beam with oscillating thickness and width (so that the profiles oscillate with different periods),
4. a periodically notched beam with non-smooth profiles (so that the mesh needs to be adapted to the singularities).

For each of these beams and each considered given circular frequency ω, a reference solution $(u_{\text{ref}}, \theta_{\text{ref}})$ is computed using the polynomial space $\mathcal{P}_9$ and a very thin mesh made of $\lceil 4\omega \rceil$ elements per unit length, *i.e.* elements of length $h = \lambda/8\pi$ for integer values of ω. For instance, for the computations performed on beams of length $L = 10$ at frequency $\omega = 5$, the reference solution is computed with $N = 200$ elements. Indeed, this refinement produced errors close to machine precision for tests performed with homogeneous and exponentially varying beams. Then, in the Lagrangian-based error $E_{\mathcal{L}}$ given by (47), the exact solution (u, θ) is replaced by this reference solution $(u_{\text{ref}}, \theta_{\text{ref}})$.

5.3.1. Beam with constant thickness and quadratically varying width

Our first example concerns a beam with rectangular cross-section and constant thickness and quadratically varying width, so that, with the scaling $A_{\text{c}} = A(0)$ and $I_{\text{c}} = I(0)$,

$$\mathcal{A}(x) = \mathcal{I}(x) = (1 + bx/L)^2, \tag{50}$$

with $b = \sqrt{\mathcal{A}(L)} - 1$. We choose $L = 10$ and $\mathcal{A}(L) = 1/8$, to obtain the beam and profiles represented in Figure 10.

This beam is very similar to the exponentially varying beam, and the results discussed above are retrieved in Figure 11, with the following differences. First, using the space $\mathcal{P}^{\omega,\alpha,\delta}_{1,8}$ instead of $\mathcal{P}^{\omega,\alpha}_{1,8}$, *i.e.* enrichment functions corresponding to exponentially varying beams instead of homogeneous beams, brings a stable improvement: the error is divided by a factor ≈ 2. A similar improvement was already observed for bars in our previous work [7]. On the other hand, the local rescaling improves a bit less the precision obtained with $\mathcal{P}^{\omega,\alpha}_{1,8}$, but still by several orders of magnitude even if the amplitude factor may not be exactly $1/\sqrt{\mathcal{A}}$.

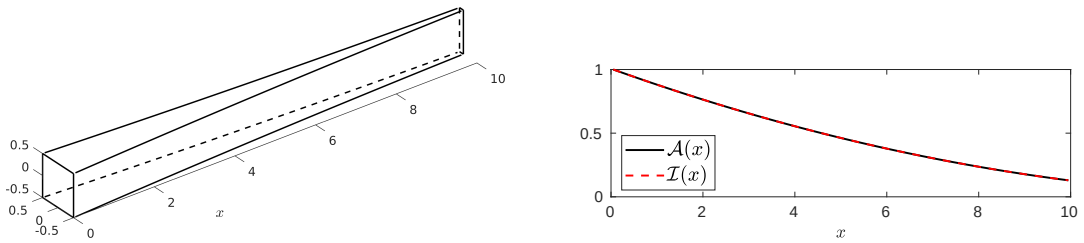

Figure 10: Beam with constant thickness and quadratic width: representation (left) and profiles (right).

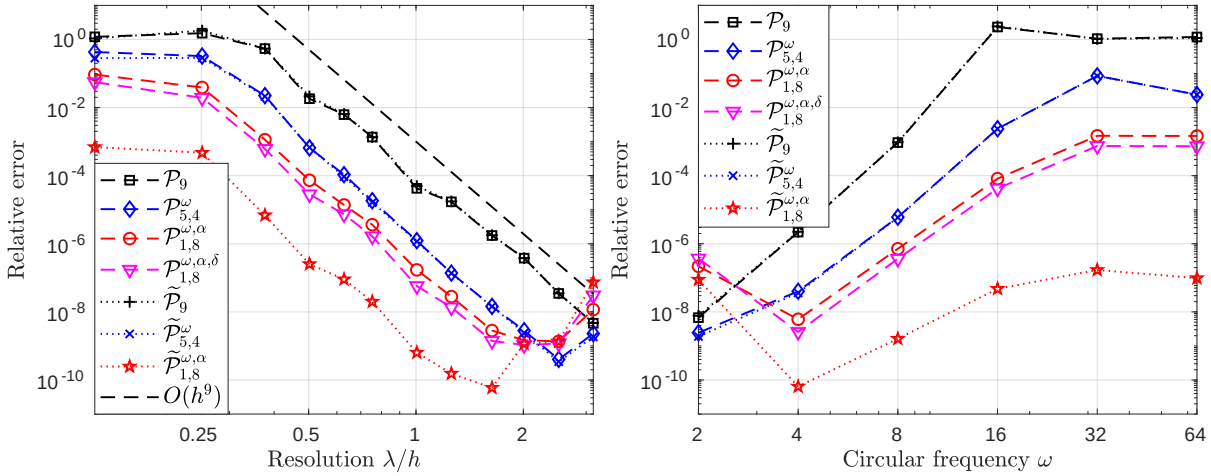

Figure 11: Relative errors for a cantilever beam with quadratic profiles represented in Figure 10 and $g = 2.5$. Left: the frequency is fixed to $\omega = 5$, and the resolution λ/h increases as the mesh is refined from 1 to 25 elements. Right: the mesh is fixed to $N = 10$ elements of length $h = 1$ and ω varies.

5.3.2. *Conical beam*

For the second example, we choose a conical beam with circular cross-section, whose radius $\bar{r}(\bar{x})$ varies linearly: $\bar{r}(\bar{x}) = \bar{r}_0 + (\bar{r}_L - \bar{r}_0)\bar{x}/\bar{L}$ for some $(\bar{r}_0, \bar{r}_L, \bar{L})$. Recalling that in this case $A = \pi\bar{r}^2$ and $I = \pi\bar{r}^4/4$, using again the scaling $A_c = A(0)$ and $I_c = I(0)$ (so that $r_c = \bar{r}_0/2$), one obtains:

$$\mathcal{A}(x) = (1 + bx/L)^2 \quad \text{and} \quad \mathcal{I}(x) = (1 + bx/L)^4, \tag{51}$$

with $b = (\bar{r}_L - \bar{r}_0)/\bar{r}_0$. We chose $L = 10$ and b such that $\mathcal{A}(L) = 1/8$ as in the previous example. The resulting beam and profiles are represented in Figure 12. Similar "tapered" beams are studied in [26, 15].

Again, we see in Figure 13 that enriched spaces perform better than the polynomial space, but for this example the gap is thinner between the Timoshenko-enriched and the sine-enriched basis spaces. The change of unknowns still does not affect the performances of the polynomial and sine-enriched spaces, but enables to gain an additional stable factor on the error (between 2 and 3) while using Timoshenko-enriched spaces.

The gap between the various errors becomes wider as the frequency increases (right panel of Figure 13), and the same remarks than for the previous example can be done: the errors obtained with enriched spaces increase more slowly than with the polynomial space, and reach a plateau for values inferior to 1% for Timoshenko-enriched space. The gain coming from the modified formulation stays noticeable but not as significant as it was for the previous example.

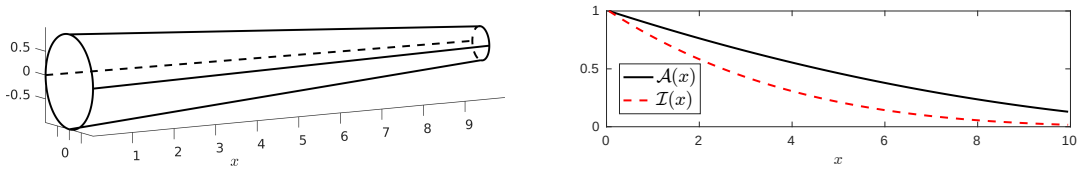

Figure 12: Conical beam with linearly varying radius: representation (left) and profiles (right).

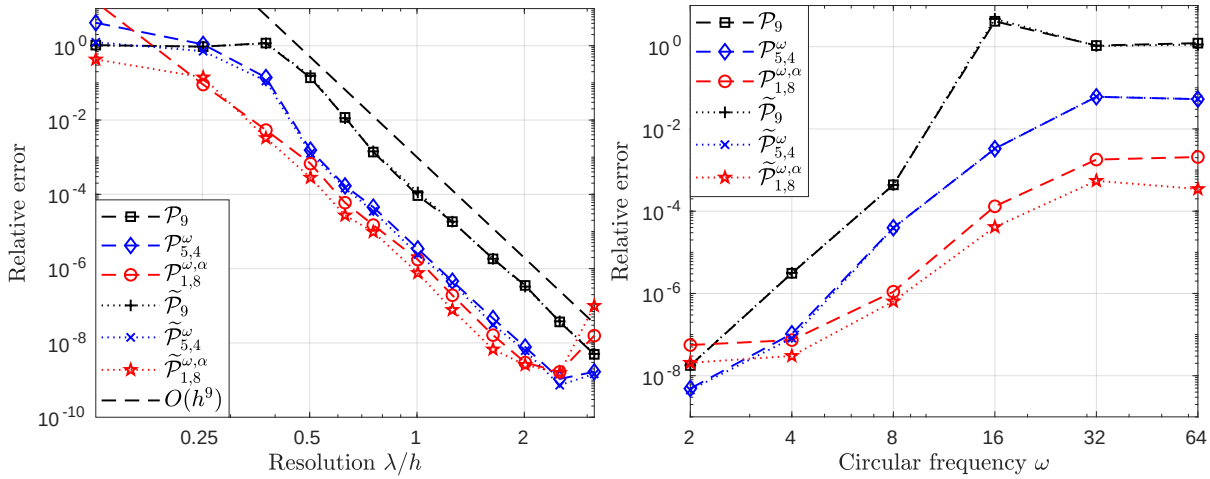

Figure 13: Relative errors for the conical cantilever beam represented in Figure 12 and $g = 2.5$. Left: the frequency is fixed to $\omega = 5$, and the resolution λ/h increases as the mesh is refined from 1 to 25 elements. Right: the mesh is fixed to $N = 10$ elements and ω varies.

5.3.3. Beam with oscillating thickness and width

We consider again a beam with rectangular cross-sections, whose profiles $\mathcal{A}$ and $\mathcal{I}$ are defined in terms of the dimensionless width b_2 and thickness b_3 as:

$$\mathcal{A}(x) = b_2(x)b_3(x) \quad \text{and} \quad \mathcal{I}(x) = b_2(x)(b_3(x))^3. \tag{52}$$

More specifically, we choose $b_2(x) = 1 - 0.5\sin(2\pi x/\ell)$ and $b_3(x) = 1 + 0.5\sin(2\pi x/\ell)$. In this way, $\mathcal{A}$ remains close to 1, while $\mathcal{I}$ oscillates with a wider amplitude as represented in Figure 14 for $L = 10$ and $\ell = 6$.

As seen in Figure 15, for the fixed low-frequency simulation the improvement brought by the enriched spaces is lower than in the previous examples. On the other hand, for this example the local rescaling improves the results obtained with all spaces: in the convergence regime the error obtained using the polynomial space (resp. enriched spaces) is reduced by a factor ≈ 2 (resp. ≈ 10).

When the mesh is fixed and the frequency increases (right panel of Figure 15), this general improvement progressively disappears and the Timoshenko-enriched space remains the only one to benefit from its association with the modified formulation, as observed on the previous examples.

5.3.4. Periodically notched beam

Our last example is a periodically notched beam represented in Figure 17, made of six straight segments and five notches with constant width and varying thickness as represented in Figure 16. This test-case in inspired by the work [37]. In this case, before the mesh definition, the beam is divided into subdomains whose boundaries match the singularities of the profiles, *i.e.* there is one subdomain per straight segment and two per notch. Then each subdomain is meshed independently.

The figure 18 illustrates the convergence rate obtained as the resolution increases for a fixed frequency $\omega = 50$ and regular meshes. A high frequency was chosen to avoid the high-resolution and badly-conditioned configurations, since regular meshes must have at least 34 elements. The expected $O(h^9)$ rate is again observed for all spaces, along with the stable improvements brought by the enrichment strategy and the rescaling.

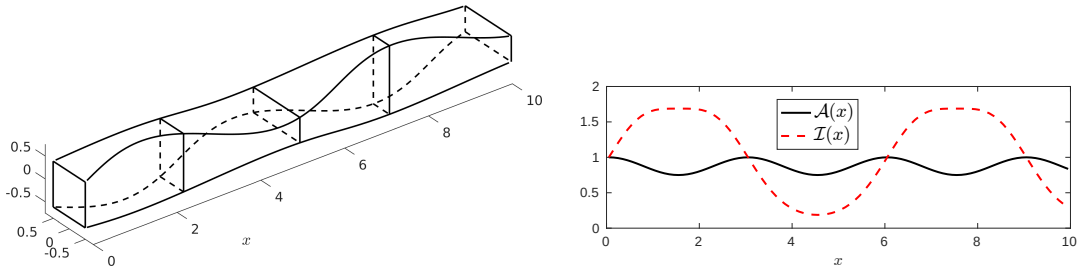

Figure 14: Beam with rectangular cross-sections and oscillating thickness and width: representation (left) and profiles (right).

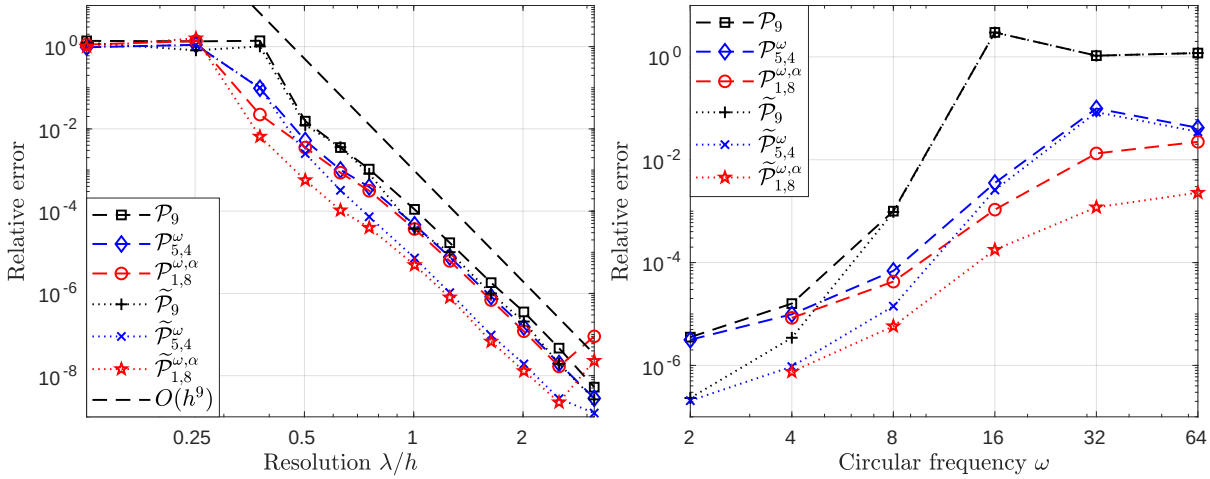

Figure 15: Relative errors for the cantilever beam with oscillating profiles represented in Figure 14 and $g = 2.5$. Left: the frequency is fixed to $\omega = 5$, and the resolution λ/h increases as the mesh is refined from 1 to 25 elements. Right: the mesh is fixed to $N = 10$ elements of length $h = 1$ and the frequency increases.

For the second example, we chose the *coarsest possible mesh* to demonstrate the capabilities of our method: each subdomain contains only one element, for a total of only $N = 16$ elements. Note that this coarse mesh is particularly justified for the straight subdomains since the *exact local solution* is then embedded in the Timoshenko-enriched basis of the space $\mathcal{P}^{\omega,\alpha}_{1,8}$. As seen in the right panel of Figure 18, the polynomial and sine-enriched spaces are largely outperformed by the Timoshenko-enriched spaces for high frequencies. Moreover, combining the modified formulation with Timoshenko-enriched bases results in a very acceptable relative error (less than 0.05%) on the whole interval of frequencies $\omega \in [2, 64]$.

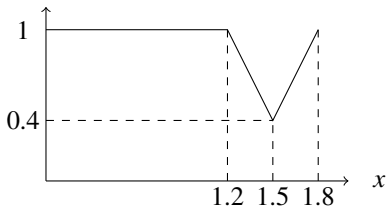

Figure 16: Variations of the thickness throughout the unit cell of the periodically notched beam.

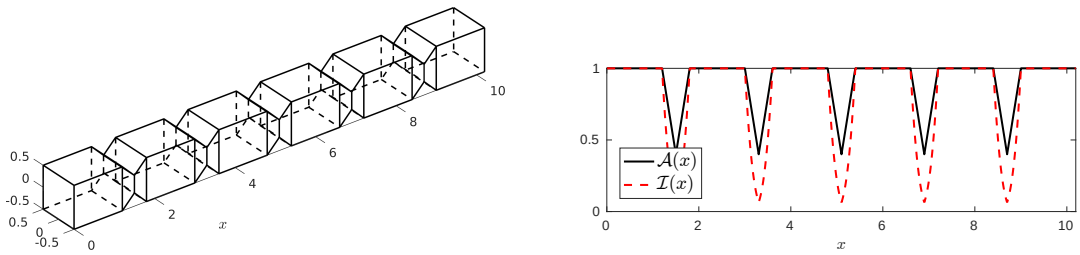

Figure 17: Periodically notched beam: representation (left) and profiles (right).

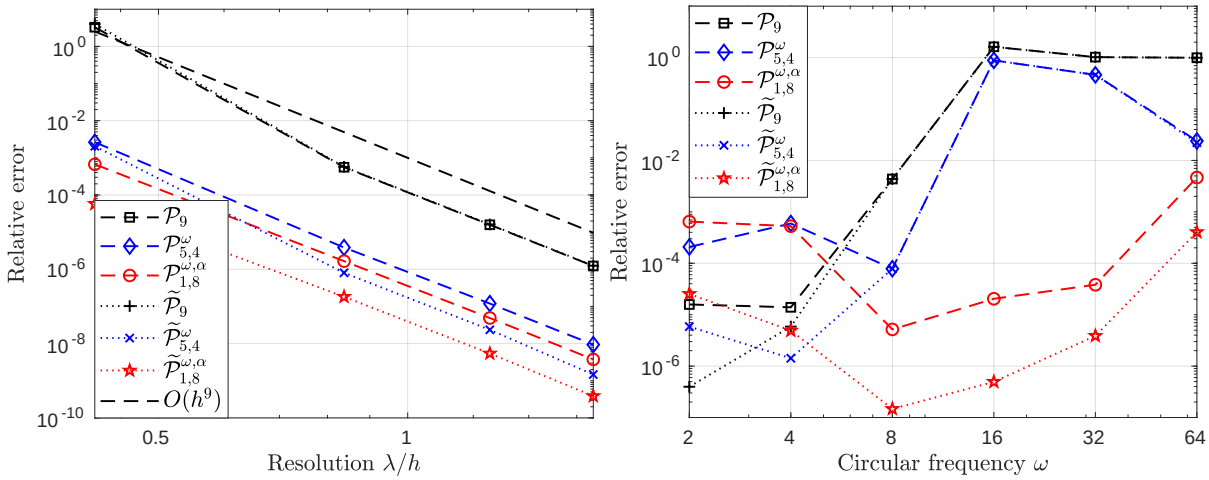

Figure 18: Relative errors for the periodically notched beam represented in Figure 17, with $g = 2.5$. Left: convergence of the error at $\omega = 50$, computed for *regular meshes* composed of $4n$ elements per straight subdomain and $2n$ elements per notch, *i.e.* $N = 34n$ and $h = 0.3/n$, with $n = 1..4$. Right: error obtained at several frequencies with the *coarsest irregular mesh*: one element of length $h_1 = 1.2$ per straight subdomain and two elements of length $h_2 = 0.3$ per notch, for a total of $N = 16$ elements.

6. Conclusions and perspectives

In this paper, we presented a finite element approach dedicated to the computation of vibrations of heterogeneous beams. More precisely, we combined (i) an enrichment method incorporating Timoshenko solutions into the approximation space and (ii) a local rescaling that accounts for the heterogeneous geometry. The resulting discrete solutions were compared with solutions obtained using classical polynomial FE spaces on several examples. With the same implementation easiness and similar computational costs, our proposal outperforms the polynomial FEM on the tested configurations. On the one hand, for a fixed frequency, all errors converge with the same rate as the mesh is refined, but using the enriched FEM improves the precision by a factor ranging from about one to several orders of magnitude depending on the considered geometry. On the other hand, our method enables to use the same coarse mesh to solve time-harmonic problems in a wide range of frequencies (several octaves), while keeping the error level at very acceptable levels (typically less than 0.1%), whereas the polynomial FEM fails to follow the fast oscillations of the solutions at high frequencies without mesh refinement.

On the theoretical side, an analysis of the method might be conduced, notably to better understand the contribution of its two components, and to predict its performances given the geometrical variations of a beam. This analysis could also reveal ways to account more precisely for this heterogeneity by building other enrichment functions, and complete our first attempts in this direction presented in Appendix A.

In parallel with these developments, the method seems robust enough already to be applied to other Timoshenko-related problems. In particular, computing natural frequencies of beams or modeling the wave propagation in the transient domain are of major interest in engineering applications. Therefore, we conclude this article by providing

some insights on the relevance of our method to tackle these problems.

Computing natural frequencies of beams. Many papers on Timoshenko beams focus on the computations of their natural frequencies. Numerous methods are proposed [14] to build stiffness and mass matrices and obtain approximations ω_h of these frequencies as the solutions of the generalized eigenvalue problem:

$$\text{Find } (\omega_h, \boldsymbol{U}) \text{ such that } (\boldsymbol{K} - \omega_h^2 \boldsymbol{M}) \cdot \boldsymbol{U} = \boldsymbol{0}. \tag{53}$$

The enriched bases presented in this work are adapted to solve vibration problems at a specific frequency ω, and therefore *a priori* seem poorly adapted to the search of natural frequencies. However, a procedure similar to the one developed for bars by Arndt et al. [2] could be investigated. Such procedure aims at determining precisely natural frequencies by (i) running an eigenfrequency search with a traditional piecewise-polynomial FE basis, and (ii) enrich the FE basis with functions corresponding to a frequency determined at step (i), to include functions close to the mode shape in the approximation space and improve the accuracy of the eigenvalue approximation for this particular frequency. Finally, the step (ii) can be repeated with the newly computed eigenfrequencies to improve the precision.

Time-domain wave propagation in Timoshenko beams. Time-domain computation can be achieved in two ways. On the one hand, a numerical scheme can be used to discretize the considered time interval. In this case, the mass matrix should be inverted at every time step. The spectral finite element method, which produces diagonal mass matrices, is particularly adapted in this case [18, 30]. Our enriched FE method, on the contrary, produces non-diagonal mass matrices; moreover it is built to be efficient for one particular frequency, thus we don't expect it to be very efficient to retrieve solutions of a time-domain problem with a wide frequency spectrum.

On the other hand, one can apply a discrete Laplace transform [1, 5] or a Fourier transform [11, 28] to the time-domain problem, then solve the resulting time-harmonic problems in the Laplace or Fourier domain for a relevant range of frequencies, and finally come back to the time-domain by an inverse transform. For this approach, the proposed enriched bases may be useful: at each frequency the computation could be accelerated by coarsening the mesh and using an appropriate enrichment, at the cost of computing the ω-dependent stiffness and mass matrices. In view of the results obtained in Section 5 for fixed meshes and increasing frequencies, one may even use the same mesh for a wide range of frequencies while keeping reasonable error levels, which could facilitate the parallelisation of the time-harmonic computations and the post-processing operations.

Acknowledgments

The authors acknowledge the support of the Centre Henri Lebesgue ANR-11-LABX-0020-01 provided through a post-doctoral fellowship to R. Cornaggia.

Appendix A. Other enriched spaces

This appendix presents other attempts made to define relevant enrichment families, that produced no noticeable improvement compared to the spaces presented in Sections 3.4 and 4.3, for the examples of Section 5.

Enrichment family resulting from the Taylor expansion of Timoshenko system for arbitrary profiles. To build relevant enrichment functions for a given equation with varying coefficients, an idea proposed by Imbert-Gérard and Després [17] (who study Helmholtz equations with variable wavenumbers) is to replace these coefficients by their Taylor expansions about the middle x_e of an element and look for the solutions of the obtained equations, called *generalized plane waves* [17]. In our case, we note $(\alpha, 2\delta, 2\beta)$ the values of the coefficients of the system (5) at the middle-point x_e (*i.e.* their 0-th order Taylor expansion):

$$\alpha = \frac{\mathcal{A}}{\mathcal{I}}(x_e), \quad 2\delta = \frac{\mathcal{A}'}{\mathcal{A}}(x_e), \quad \text{and} \quad 2\beta = \frac{\mathcal{I}'}{\mathcal{I}}(x_e), \tag{A.1}$$

and keeping only these leading-order contributions in the equations (5), the resulting system is:

$$\begin{cases} -\omega^2 u = 2\delta(u' - \theta) + (u' - \theta)' \\ -\omega^2 \theta = \alpha(u' - \theta) + g\,(2\beta\theta' + \theta'')\,. \end{cases} \tag{A.2}$$

Note that this system *does not correspond to an actual beam* when $\delta \neq \beta$ and therefore its relevance is hard to determine using physical insights. The dispersion relation is found to be:

$$(\omega^2 - (k^2 - 2\mathrm{i}\delta k))(\omega^2 - g(k^2 - 2\mathrm{i}\beta k) - \alpha) - \alpha(k^2 - 2\mathrm{i}\delta k) = 0, \tag{A.3}$$

or:

$$gk^4 - 2g\mathrm{i}(\delta + \beta)k^3 - (\omega^2(1 + g) + 4g\delta\beta)k^2 + 2\mathrm{i}\omega^2(\delta + g\beta)k + \omega^2(\omega^2 - \alpha) = 0. \tag{A.4}$$

We found no closed-form expression of the roots $\{\bar{k}_m\}_{m=1\ldots4}$ of this equation, but they may be computed numerically for each set of parameters $(\omega, \alpha, \delta, \beta)$, and the basis of solutions is then given by:

$$\Psi^{\omega,\alpha,\delta,\beta} = \left\{x \mapsto e^{\mathrm{i}\bar{k}_m x}\right\}_{m=1..4}. \tag{A.5}$$

This family was used to build a space $\mathcal{P}_{1,8}^{\omega,\alpha,\delta,\beta}$ similar to $\mathcal{P}_{1,8}^{\omega,\alpha}$ and $\mathcal{P}_{1,8}^{\omega,\alpha,\delta}$, for which the e-th elementary basis is determined from the values of (α, δ, β) computed with (A.1). However, no significant improvement was observed compared to the simpler space $\mathcal{P}_{1,8}^{\omega,\alpha}$, and compared to $\mathcal{P}_{1,8}^{\omega,\alpha,\delta}$ for beams with constant thickness.

We applied the same idea to the system (41) obtained after the change of unknowns $(u, \theta) \to (\tilde{u}, \tilde{\theta})$. By retaining only the middle-point values of all the variable coefficients (d''/d, d'/a, …), writing the dispersion relation of the resulting system and computing its roots, one may define a new family $\Psi^{\omega,d,a}$ of enrichment functions and build the corresponding space $\widetilde{\mathcal{P}}_{1,8}^{\omega,d,a}$ similarly than above. This space was used instead of $\widetilde{\mathcal{P}}_{1,8}^{\omega,\alpha}$ to discretize the modified formulation (42), but again, no clear improvement was observed.

Enrichments inspired by the Stable generalized FEM. Given an enrichment family $\{\psi_m\}$, there are alternative ways to add inner functions (*i.e.* functions that vanish at both nodes of the element) to an elementary basis. In particular, we borrowed one of the ideas of the Stable GFEM [3] for which the linear interpolant of the enrichment functions is subtracted from these functions on each element. We built alternative Timoshenko-enriched spaces $\mathcal{P}_{5,4}^{\omega,\alpha}$, for which only four additional inner functions are added to a fifth-order polynomial basis. These functions read:

$$\overline{\varphi_e^m}(\xi) = e^{\mathrm{i}k_m h_e \xi} - 1 - \xi(e^{\mathrm{i}k_m h_e} - 1), \quad m = 1\,..\,4, \tag{A.6}$$

where the wavenumbers k_m are defined by (12). In particular, we expected such bases to produce better-conditioned systems (as each enrichment function appears only once in the elementary basis). However, on the examples presented in Section 5, these spaces were found to perform poorly compared to the spaces $\mathcal{P}_{1,8}^{\omega,\alpha}$, that uses the same enrichment functions but multiplied by the "half-hat" local PU.

Appendix B. An exact solution for nonzero density of forces

For an exponential beam, a particular solution of the Timoshenko system (5) is sought by imposing $u_{\mathrm{P}}(x) = (x/L)^2$ and $m(x) = 0$. Then the unknown rotation θ_{P} and density of forces $q_{\mathrm{P}}(x) = \mathcal{A}(x)\bar{q}_{\mathrm{P}}(x)$ are the solutions of the system:

$$\begin{cases} 2 - \theta_{\mathrm{P}}' + 2\delta(u_{\mathrm{P}}' - \theta_{\mathrm{P}}) + \omega^2 u_{\mathrm{P}} + \bar{q}_{\mathrm{P}} = 0 \\ g\,(\theta_{\mathrm{P}}'' + 2\delta\theta_{\mathrm{P}}') + \alpha(u_{\mathrm{P}}' - \theta_{\mathrm{P}}) + \omega^2\theta_{\mathrm{P}} = 0. \end{cases} \tag{B.1}$$

The rotation θ_{P} and the force density q_{P} are determined successively thanks to the second and the first equation. Finally, the particular solution

$$u_{\mathrm{P}}(x) = \frac{x^2}{L^2}, \qquad \theta_{\mathrm{P}}(x) = \frac{1}{L^2}\frac{2\alpha}{\alpha - \omega^2}\left(x + \frac{2g\delta}{\alpha - \omega^2}\right) \tag{B.2}$$

is obtained by imposing the linear density of forces:

$$q_{\mathrm{P}}(x) = \mathcal{A}(x)\bar{q}_{\mathrm{P}}(x) = \frac{e^{2\delta x}}{L^2}\left[-\omega^2 x^2 + \frac{2}{\alpha - \omega^2}\left(2\delta\omega^2 x + \omega^2 + \frac{4g\alpha\delta^2}{\alpha - \omega^2}\right)\right]. \tag{B.3}$$

References

[1] V. Adàmek and F. Valeš. Analytical solution for a heterogeneous Timoshenko beam subjected to an arbitrary dynamic transverse load. *European Journal of Mechanics - A/Solids*, 49:373 – 381, 2015.

[2] M. Arndt, R. Machado, and A. Scremin. An adaptive generalized finite element method applied to free vibration analysis of straight bars and trusses. *Journal of Sound and Vibration*, 329(6):659 – 672, 2010.

[3] I. Babuška and U. Banerjee. Stable generalized finite element method (SGFEM). *Computer Methods in Applied Mechanics and Engineering*, 201-204:91–111, 2012.

[4] I. Babuška and Z. Zhang. The partition of unity method for the elastically supported beam. *Computer Methods in Applied Mechanics and Engineering*, 152(1):1 – 18, 1998.

[5] F. F. Calim. Transient analysis of axially functionally graded Timoshenko beams with variable cross-section. *Composites Part B: Engineering*, 98:472 – 483, 2016.

[6] W. Cleghorn and B. Tabarrok. Finite element formulation of a tapered Timoshenko beam for free lateral vibration analysis. *Journal of Sound and Vibration*, 152(3):461 – 470, 1992.

[7] R. Cornaggia, E. Darrigrand, L. Le Marrec, and F. Mahé. Enriched finite elements for time-harmonic Webster's equation. *Computer Methods in Applied Mechanics and Engineering*, 341:985 – 1007, 2018.

[8] M. Eisenberger. Dynamic stiffness matrix for variable cross-section Timoshenko beams. *Communications in Numerical Methods in Engineering*, 11(6):507–513, 1995.

[9] A. Ern and J.-L. Guermond. *Theory and practice of finite elements*, volume 159. Springer Science & Business Media, 2004.

[10] C. Forgit, B. Lemoine, L. Le Marrec, and L. Rakotomanana. A Timoshenko-like model for the study of three-dimensional vibrations of an elastic ring of general cross-section. *Acta Mechanica*, 227(9):2543–2575, Sep 2016.

[11] S. Gopalakrishnan, M. Martin, and J. Doyle. A matrix methodology for spectral analysis of wave propagation in multiple connected Timoshenko beams. *Journal of Sound and Vibration*, 158(1):11 – 24, 1992.

[12] K. F. Graff. *Wave motion in elastic solids*. Oxford University Press, 1975.

[13] F. Gruttmann and W. Wagner. Shear correction factors in Timoshenko's beam theory for arbitrary shaped cross-sections. *Computational Mechanics*, 27(3):199–207, Mar 2001.

[14] M. Hajianmaleki and M. S. Qatu. Vibrations of straight and curved composite beams: A review. *Composite Structures*, 100:218 – 232, 2013.

[15] Y. Huang, L.-E. Yang, and Q.-Z. Luo. Free vibration of axially functionally graded Timoshenko beams with non-uniform cross-section. *Composites Part B: Engineering*, 45(1):1493 – 1498, 2013.

[16] F. Ihlenburg. *Finite Element Analysis of Acoustic Scattering*. Springer Publishing Company, Incorporated, 1998.

[17] L.-M. Imbert-Gérard and B. Després. A generalized plane-wave numerical method for smooth nonconstant coefficients. *IMA Journal of Numerical Analysis*, 34(3):1072–1103, 2014.

[18] P. Kudela, M. Krawczuk, and W. Ostachowicz. Wave propagation modelling in 1d structures using spectral finite elements. *Journal of Sound and Vibration*, 300(1-2):88 – 100, 2007.

[19] L. Li. Discretization of the Timoshenko beam problem by the p and the h-p versions of the finite element method. *Numerische Mathematik*, 57(1):413–420, 1990.

[20] J. Melenk and I. Babuška. The partition of unity finite element method: Basic theory and applications. *Computer Methods in Applied Mechanics and Engineering*, 139(1):289 – 314, 1996.

[21] N. Olhoff, B. Niu, and G. Cheng. Optimum design of band-gap beam structures. *International Journal of Solids and Structures*, 49(22):3158–3169, nov 2012.

[22] M. Ostoja-Starzewski and A. Woods. Spectral finite elements for vibrating rods and beams with random field properties. *Journal of Sound and Vibration*, 268(4):779 – 797, 2003.

[23] J. Reddy. On locking-free shear deformable beam finite elements. *Computer Methods in Applied Mechanics and Engineering*, 149(1):113 – 132, 1997. Containing papers presented at the Symposium on Advances in Computational Mechanics.

[24] S. W. Rienstra. Webster's horn equation revisited. *SIAM Journal on Applied Mathematics*, 65(6):1981–2004, 2005.

[25] K. Sarkar and R. Ganguli. Closed-form solutions for axially functionally graded Timoshenko beams having uniform cross-section and fixed-fixed boundary condition. *Composites Part B: Engineering*, 58:361 – 370, 2014.

[26] A. Shahba, R. Attarnejad, M. T. Marvi, and S. Hajilar. Free vibration and stability analysis of axially functionally graded tapered Timoshenko beams with classical and non-classical boundary conditions. *Composites Part B: Engineering*, 42(4):801 – 808, 2011.

[27] Y. Shang Hsu. Enriched finite element methods for Timoshenko beam free vibration analysis. *Applied Mathematical Modelling*, 40(15):7012 – 7033, 2016.

[28] W. Shen, D. Li, S. Zhang, and J. Ou. Analysis of wave motion in one-dimensional structures through fast-Fourier-transform-based wavelet finite element method. *Journal of Sound and Vibration*, 400:369 – 386, 2017.

[29] F. Sohani and H. R. Eipakchi. Analytical solution for modal analysis of Euler-bernoulli and Timoshenko beam with an arbitrary varying cross-section. *Mathematical Models in Engineering*, 4(3):164–174, sep 2018.

[30] M. A. Sprague and T. L. Geers. Legendre spectral finite elements for structural dynamics analysis. *Communications in Numerical Methods in Engineering*, 24(12):1953–1965, 2008.

[31] T. Strouboulis, I. Babuška, and K. Copps. The design and analysis of the generalized finite element method. *Computer Methods in Applied Mechanics and Engineering*, 181(1-3):43 – 69, 2000.

[32] C.-Y. Tai and Y. Chan. A hierarchic high-order Timoshenko beam finite element. *Computers & Structures*, 165:48–58, 2016.

[33] A.-Y. Tang, J.-X. Wu, X.-F. Li, and K. Lee. Exact frequency equations of free vibration of exponentially non-uniform functionally graded Timoshenko beams. *International Journal of Mechanical Sciences*, 89:1 – 11, 2014.

[34] X. Tong, B. Tabarrok, and K. Yeh. Vibration analysis of Timoshenko beams with non-homogeneity and varying cross-section. *Journal of Sound and Vibration*, 186(5):821 – 835, 1995.

[35] Z. Wang, X. Wang, G. Xu, S. Cheng, and T. Zeng. Free vibration of two-directional functionally graded beams. *Composite Structures*, 135:191 – 198, 2016.

[36] J. Yuan, Y.-H. Pao, and W. Chen. Exact solutions for free vibrations of axially inhomogeneous Timoshenko beams with variable cross section. *Acta Mechanica*, 227(9):2625–2643, 2016.

[37] A. Żak, M. Krawczuk, M. Palacz, L. Doliński, and W. Waszkowiak. High frequency dynamics of an isotropic Timoshenko periodic beam by the use of the time-domain spectral finite element method. *Journal of Sound and Vibration*, 409:318 – 335, 2017.

[38] D. Zhou and Y. K. Cheung. Vibrations of tapered Timoshenko beams in terms of static Timoshenko beam functions. *ASME. J. Appl. Mech.*, 2000.